Dynamics of Lithosphere-Mantle Coupling: Global Stress and Plate Motions

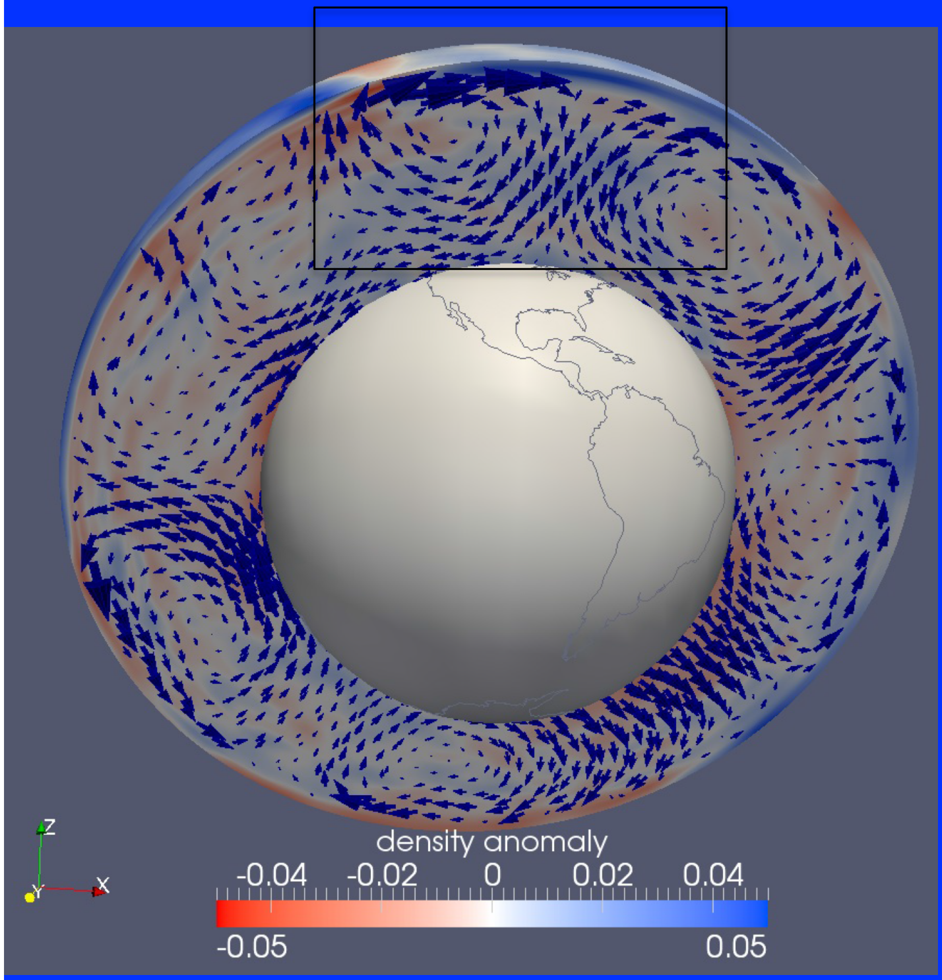

William E. Holt[1], Attreyee Ghosh[2], Xinguo Wang[3], Lianxing Wen[1]

[1]Department of Geosciences, Stony Brook University

[2]Center for Earth Sciences, Indian Institute of Sciences

[3]Institute of Tibetan Plateau Research Chinese Academy of Sciences

Global Modeling of Lithosphere Stress and Plate Motion

- What is the total stress energy in the plate tectonic system?
- How much arises from GPE of the lithosphere and how much from coupling with mantle?
- What are the implications for strength profiles and possible role of weakening mechanisms?
- Calibration of present-day forces places important constraints on models that address geologic time scale evolution with feedbacks

Force Balance Equations in spherical coordinates

$$\frac{1}{\cos\theta}\frac{\partial}{\partial\varphi}\left(r^2\sigma_{\varphi\varphi}\right)+\frac{1}{\cos^2\theta}\frac{\partial}{\partial\theta}\left(r^2\sigma_{\varphi\theta}\cos^2\theta\right)+\frac{\partial}{\partial r}\left(r^3\sigma_{\varphi r}\right)=0 \quad (1)$$

$$\begin{aligned}\frac{1}{\cos\theta}\frac{\partial}{\partial\varphi}\left(r^2\sigma_{\varphi\theta}\right)&+\frac{1}{2}\frac{\partial}{\partial\theta}\left(r^2\left[\sigma_{\theta\theta}+\sigma_{\varphi\varphi}\right]\right)\\&+\frac{1}{2\cos^2\theta}\frac{\partial}{\partial\theta}\left(r^2\cos^2\theta\left[\sigma_{\theta\theta}-\sigma_{\varphi\varphi}\right]\right)\\&+\frac{\partial}{\partial r}\left(r^3\sigma_{\theta r}\right)=0 \quad (2)\end{aligned}$$

$$\begin{aligned}\frac{1}{r\cos\theta}\frac{\partial\sigma_{\varphi r}}{\partial\varphi}&+\frac{1}{r\cos\theta}\frac{\partial}{\partial\theta}\left(\cos\theta\sigma_{\theta r}\right)+\frac{1}{r}\left(2\sigma_{rr}-\sigma_{\varphi\varphi}-\sigma_{\theta\theta}\right)\\&+\frac{\partial\sigma_{rr}}{\partial r}-\rho g=0 \quad (3)\end{aligned}$$

Vertically integrating (1) and (2) and substituting: $\sigma_{ij} = \tau_{ij} + \frac{1}{3}\,\sigma_{kk}\delta_{ij}$

$$\frac{1}{\cos\theta}\frac{\partial}{\partial\varphi}\left(\int_{r_L}^{r_0} r^2\tau_{\varphi\varphi}\mathrm{d}r\right) - \frac{1}{\cos\theta}\frac{\partial}{\partial\varphi}\left(\int_{r_L}^{r_0} r^2\tau_{rr}\mathrm{d}r\right) + \frac{1}{\cos^2\theta}\frac{\partial}{\partial\theta}\left(\cos^2\theta\int_{r_L}^{r_0} r^2\tau_{\varphi\theta}\mathrm{d}r\right)$$

$$= -\frac{1}{\cos\theta}\frac{\partial}{\partial\varphi}\left(\int_{r_L}^{r_0} r^2\sigma_{rr}\mathrm{d}r\right) - r_0^3\tau_{\varphi r}(r_0) + r_L^3\tau_{\varphi r}(r_L) \qquad (4)$$

and

$$\frac{1}{\cos\theta}\frac{\partial}{\partial\varphi}\left(\int_{r_L}^{r_0} r^2\tau_{\varphi\theta}\mathrm{d}r\right) + \frac{1}{2}\frac{\partial}{\partial\theta}\left(\int_{r_L}^{r_0} r^2\tau_{\theta\theta}\mathrm{d}r + \int_{r_L}^{r_0} r^2\tau_{\varphi\varphi}\mathrm{d}r\right) + \frac{\partial}{\partial\theta}\left(\int_{r_L}^{r_0} r^2\tau_{rr}\mathrm{d}r\right)$$

$$+ \frac{1}{2\cos^2\theta}\frac{\partial}{\partial\theta}\left(\cos^2\theta\left[\int_{r_L}^{r_0} r^2\tau_{\theta\theta}\mathrm{d}r - \int_{r_L}^{r_0} r^2\tau_{\varphi\varphi}\mathrm{d}r\right]\right)$$

$$= -\frac{\partial}{\partial\theta}\left(\int_{r_L}^{r_0} r^2\sigma_{rr}\mathrm{d}r\right) - r_0^3\tau_{\theta r}(r_0) + r_L^3\tau_{\theta r}(r_L) \qquad (5)$$

[8] The approximation that we make, which could be called the approximation that underlies the "thin sheet" approach, is that the gradients of $\sigma_{\varphi r}$ and $\sigma_{\theta r}$ in equation (3) are negligibly small as is the term $\frac{1}{r}\left(2\sigma_{rr} - \sigma_{\varphi\varphi} - \sigma_{\theta\theta}\right)$ compared to ρg. Hence, equation (3) can be approximated as

$$\sigma_{rr} = -\int_{r}^{r_0} \rho g \mathrm{d}r, \tag{6}$$

so that the GPE equation is given by

$$\begin{aligned}\int_{r_L}^{r_0} r^2 \sigma_{rr} \mathrm{d}r &= -\int_{r_L}^{r_0} r^2 \left[\int_{r}^{r_0} \rho g \mathrm{d}r'\right] \mathrm{d}r \\ &= -\int_{r_L}^{r_0} \rho g \left[\int_{r_L}^{r'} r^2 \mathrm{d}r\right] \mathrm{d}r' \\ &= -\int_{r_L}^{r_0} \frac{1}{3} \rho g \left(r'^3 - r_L^3\right) \mathrm{d}r' \end{aligned} \tag{7}$$

Global Modeling of Lithosphere Stress and Plate Motion

- Lithosphere calculations:
  - Depth integrated 3-D force balance equations in a lithosphere shell
  - Solved using finite element global method
    - Weak formulation
    - Higher order elements in quadrilateral grid (Code written by A.J. Haines)
  - Internal body forces (GPE), and basal traction boundary conditions (Mantle Convection)

Method Applied Regionally and Globally

- **Applied to Western U.S. and Central Asia without basal tractions:**

- Flesch, L. M., W. E. Holt, A. J. Haines, and B. Shen-Tu (2000), The dynamics of the Pacific-North America plate boundary zone in the Western U. S., *Science*, *287*, 834-836, 2000.
- Flesch, L.M., Haines, A. J., and W. E. Holt (2001), The dynamics of the India-Eurasia Collision Zone*, J. Geophys. Res., 106*, 16,435-16,460, 2001.

- **Applied globally with contribution from lithosphere only**:

- Ghosh, A., W. E. Holt, and L. M. Flesch (2009), Contribution of Gravitational Potential Energy Differences to the Global Stress Field, *Geophys. Jour. Int*., doi: 10.1111/j.1365-246X.2009.04326.x

- **Applied globally with mantle flow and lithosphere contributions:**

- Ghosh, A., W. E. Holt, L. Wen, A. J. Haines, and L. M. Flesch (2008), Joint modeling of lithosphere and mantle dynamics elucidating lithosphere-mantle coupling, *Geophys. Res. Lett*., 35, L16309, doi:10.1029/2008GL034365
- Ghosh, A., and W. E. Holt (2012), Plate Motions and Stresses from Global Dynamic Models (2012), *Science*, 335, doi:10.1126/science.1214209,
- Ghosh, A., W. E. Holt, and L. M. Wen (2013), Predicting the lithospheric stress field and plate motions by joint modeling of lithosphere and mantle dynamics, *J. Geophys. Res: Solid Earth*, 118, doi:10.1029/2012JB009516.

Vertically integrating (1) and (2) and substituting: $\sigma_{ij} = \tau_{ij} + \frac{1}{3}\,\sigma_{kk}\delta_{ij}$

$$\frac{1}{\cos\theta}\frac{\partial}{\partial\varphi}\left(\int_{r_L}^{r_0} r^2\tau_{\varphi\varphi}\mathrm{d}r\right) - \frac{1}{\cos\theta}\frac{\partial}{\partial\varphi}\left(\int_{r_L}^{r_0} r^2\tau_{rr}\mathrm{d}r\right) + \frac{1}{\cos^2\theta}\frac{\partial}{\partial\theta}\left(\cos^2\theta\int_{r_L}^{r_0} r^2\tau_{\varphi\theta}\mathrm{d}r\right)$$

$$= -\frac{1}{\cos\theta}\frac{\partial}{\partial\varphi}\left(\int_{r_L}^{r_0} r^2\sigma_{rr}\mathrm{d}r\right) - r_0^3\tau_{\varphi r}(r_0) + r_L^3\tau_{\varphi r}(r_L) \qquad (4)$$

and

$$\frac{1}{\cos\theta}\frac{\partial}{\partial\varphi}\left(\int_{r_L}^{r_0} r^2\tau_{\varphi\theta}\mathrm{d}r\right) + \frac{1}{2}\frac{\partial}{\partial\theta}\left(\int_{r_L}^{r_0} r^2\tau_{\theta\theta}\mathrm{d}r + \int_{r_L}^{r_0} r^2\tau_{\varphi\varphi}\mathrm{d}r\right) + \frac{\partial}{\partial\theta}\left(\int_{r_L}^{r_0} r^2\tau_{rr}\mathrm{d}r\right)$$

$$+ \frac{1}{2\cos^2\theta}\frac{\partial}{\partial\theta}\left(\cos^2\theta\left[\int_{r_L}^{r_0} r^2\tau_{\theta\theta}\mathrm{d}r - \int_{r_L}^{r_0} r^2\tau_{\varphi\varphi}\mathrm{d}r\right]\right)$$

$$= -\frac{\partial}{\partial\theta}\left(\int_{r_L}^{r_0} r^2\sigma_{rr}\mathrm{d}r\right) - r_0^3\tau_{\theta r}(r_0) + r_L^3\tau_{\theta r}(r_L) \qquad (5)$$

Minimize Functional, *I*, with respect to Lagrange multipliers

$$I = \iint \frac{1}{\mu}\left[\bar{\tau}^2_{\varphi\varphi} + 2\bar{\tau}^2_{\varphi\theta} + \bar{\tau}^2_{\theta\theta} + \left(\bar{\tau}_{\varphi\varphi} + \bar{\tau}_{\theta\theta}\right)^2\right]\cos\theta \mathrm{d}\varphi \mathrm{d}\theta$$

$$+ \iint \left\{ 2\lambda_\varphi \left[\frac{1}{\cos\theta}\frac{\partial \bar{\tau}_{\varphi\varphi}}{\partial\varphi} + \frac{1}{\cos\theta}\frac{\partial}{\partial\varphi}\left(\bar{\tau}_{\varphi\varphi} + \bar{\tau}_{\theta\theta}\right)\right.\right.$$

$$\left. + \frac{1}{\cos^2\theta}\frac{\partial}{\partial\theta}\left(\cos^2\theta\,\bar{\tau}_{\varphi\theta}\right) + \frac{1}{\cos\theta}\frac{\partial\bar{\sigma}_{rr}}{\partial\varphi} - r_L^3\sigma_{\varphi r}(r_L)\right]$$

$$+ 2\lambda_\theta\left[\frac{1}{\cos\theta}\frac{\partial\bar{\tau}_{\varphi\theta}}{\partial\varphi} + \frac{3}{2}\frac{\partial}{\partial\theta}\left(\bar{\tau}_{\theta\theta} + \bar{\tau}_{\varphi\varphi}\right)\right.$$

$$+ \frac{1}{2\cos^2\theta}\frac{\partial}{\partial\theta}\left(\cos^2\theta\left[\bar{\tau}_{\theta\theta} - \bar{\tau}_{\varphi\varphi}\right]\right)$$

$$\left.\left. + \frac{\partial\bar{\sigma}_{rr}}{\partial\theta} - r_L^3\sigma_{\theta r}(r_L)\right]\right\}\cos\theta d\varphi d\theta$$

Relation between deviatoric stress and Lagrange multipliers

$$\bar{\tau}_{\varphi\varphi} = \mu\left(\frac{1}{\cos\theta}\frac{\partial\lambda_\varphi}{\partial\varphi} - \lambda_\theta \tan\theta\right),$$

$$\bar{\tau}_{\theta\theta} = \mu\frac{\partial\lambda_\theta}{\partial\theta},$$

$$\bar{\tau}_{\varphi\theta} = \frac{\mu}{2}\left(\frac{\partial\lambda_\varphi}{\partial\theta} + \frac{1}{\cos\theta}\frac{\partial\lambda_\theta}{\partial\varphi} + \lambda_\varphi \tan\theta\right).$$

Relation with deviatoric stress and Lagrange multipliers is the same as the relation between strain rate and velocities

Lagrange multipliers are zero along the boundaries (circular rings at 88° N, 88° S)

Substitute expressions in for deviatoric stress and minimize J functional with respect to Lagrange multipliers. This provides solution to force balance equations.

$$J = \iint \left\{ \left[\begin{pmatrix} \bar{\tau}_{\varphi\varphi} \\ \bar{\tau}_{\theta\theta} \\ \bar{\tau}_{\varphi\theta} \end{pmatrix} - \begin{pmatrix} \Phi^{obs}_{\varphi\varphi} \\ \Phi^{obs}_{\theta\theta} \\ \Phi^{obs}_{\varphi\theta} \end{pmatrix} \right]^T \widetilde{V}^{-1} \left[\begin{pmatrix} \bar{\tau}_{\varphi\varphi} \\ \bar{\tau}_{\theta\theta} \\ \bar{\tau}_{\varphi\theta} \end{pmatrix} - \begin{pmatrix} \Phi^{obs}_{\varphi\varphi} \\ \Phi^{obs}_{\theta\theta} \\ \Phi^{obs}_{\varphi\theta} \end{pmatrix} \right] \right\} \cos\theta \mathrm{d}\varphi \mathrm{d}\theta .$$

The potentials are composed of horizontal integrals of the body force equivalents

Constraints for Effective Forces

Density structure:
- Crust 2.0 in lithosphere; also cooling plate model [Stein & Stein, 1992].

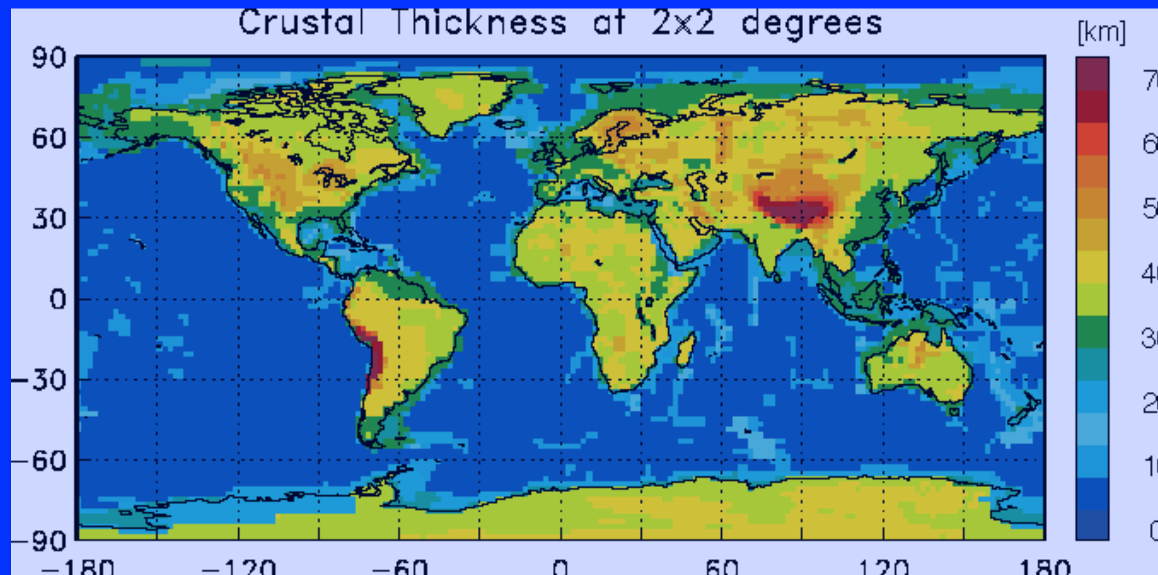

- Mantle tomography and history of subduction models

−750

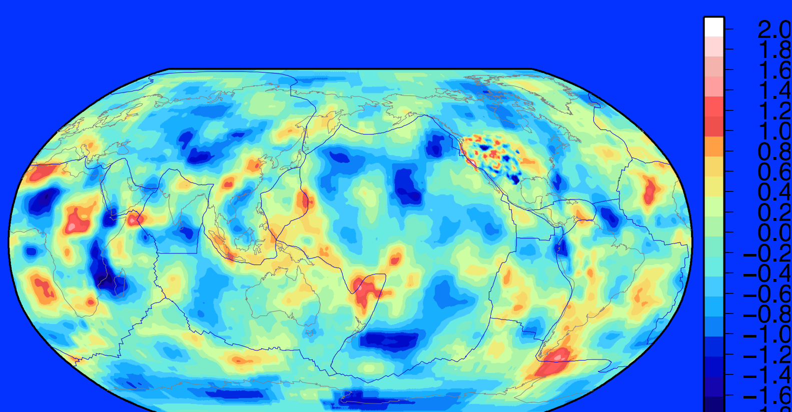

−810

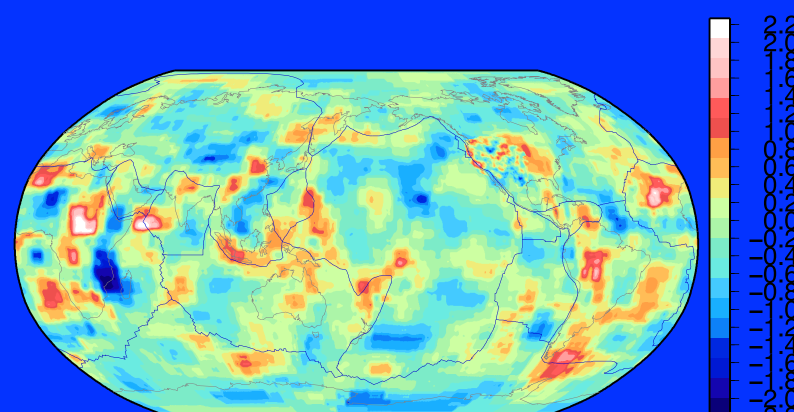

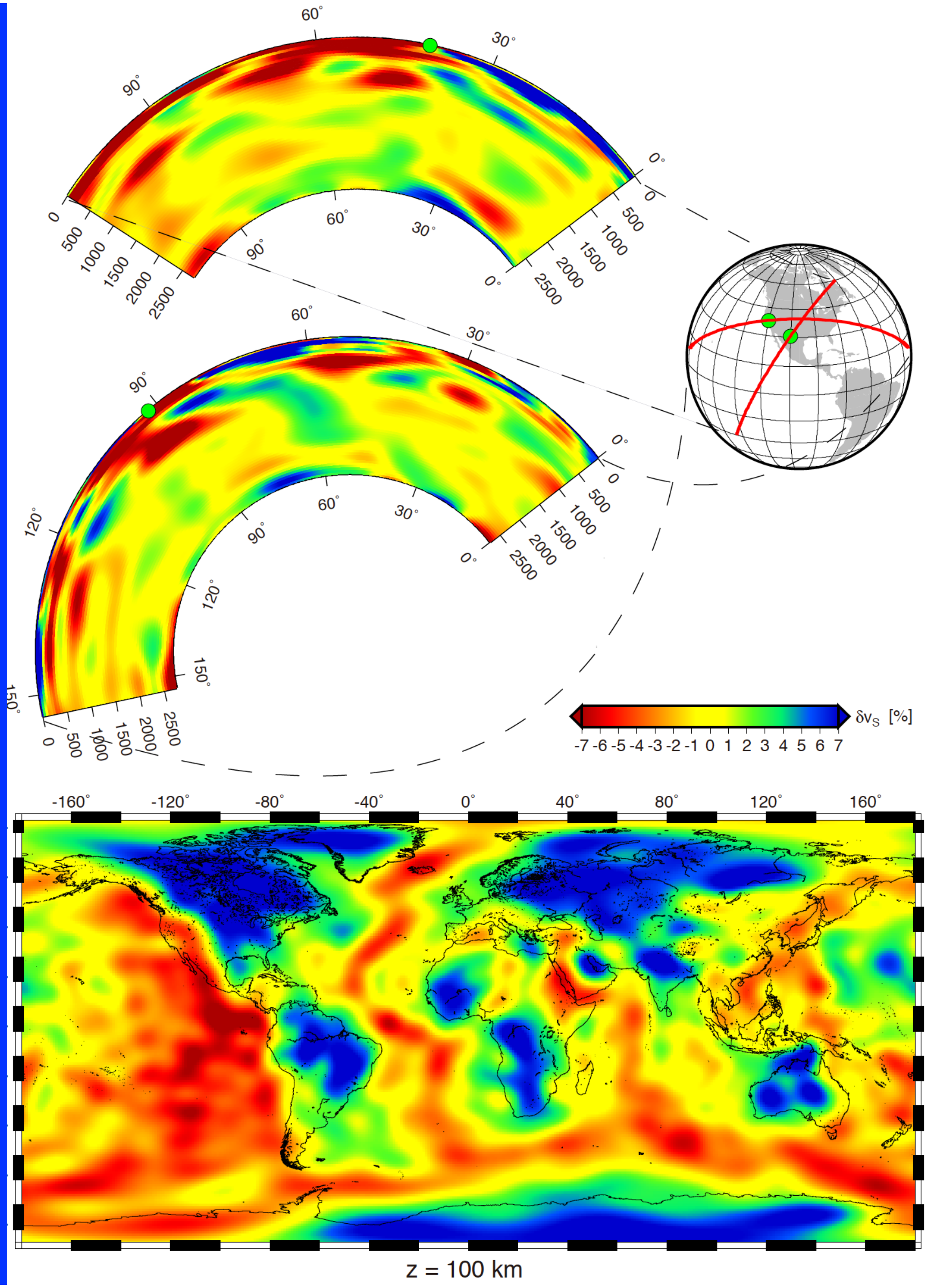

Example of tomography model

Lekic and Romanowicz [2011] *Geophys. J. Int.*

Farallon plate subduction history impacts North America dynamics

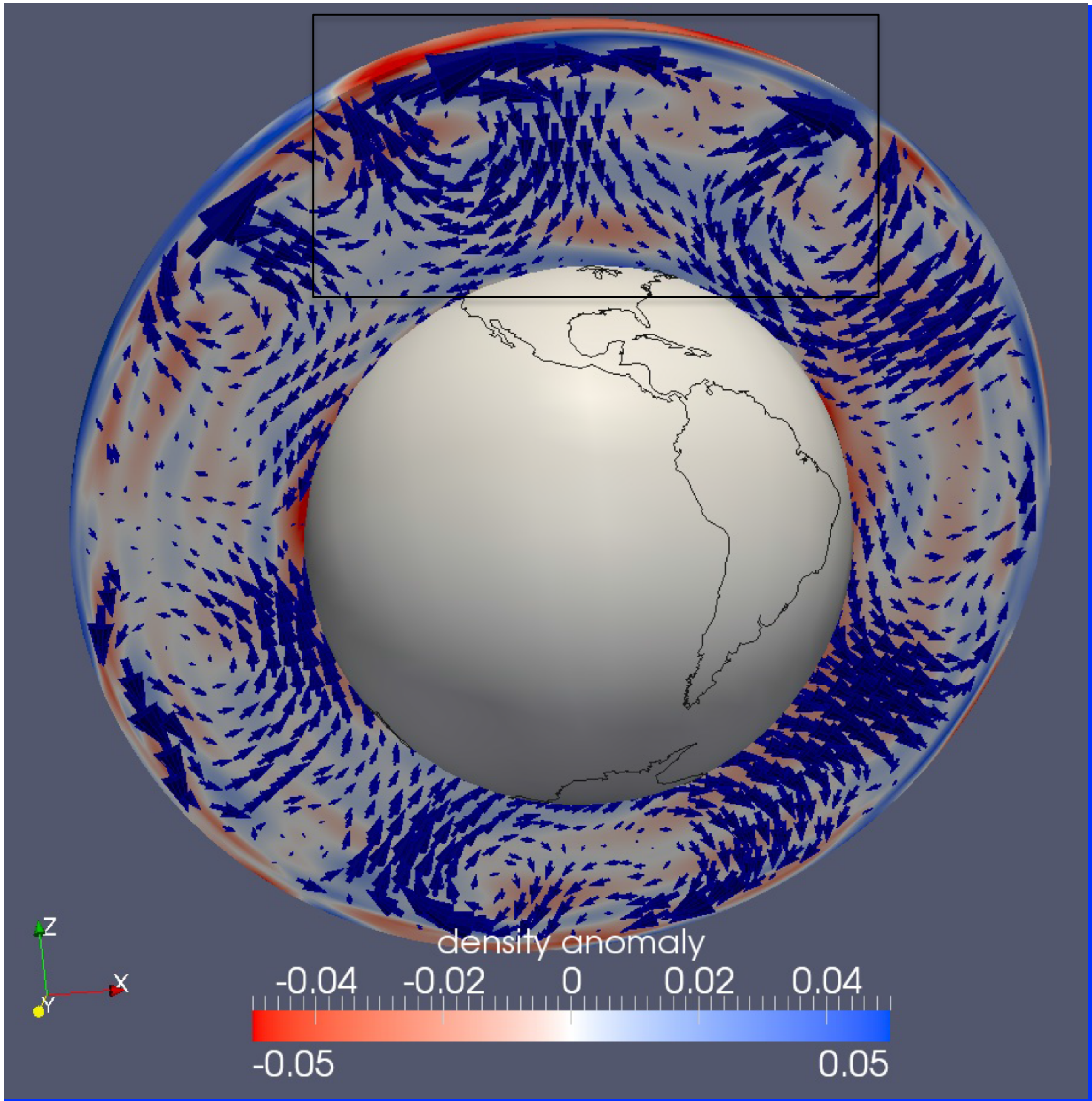

Another Example

Tomography model from*: Ritsema, Deuss, van Heijst, & Woodhouse* [2011] *Geophys. J. Int*.
Computed using HC Code [*Milner et al.*, 2009] *Eos*

Benchmarking with 3-D spherical convection

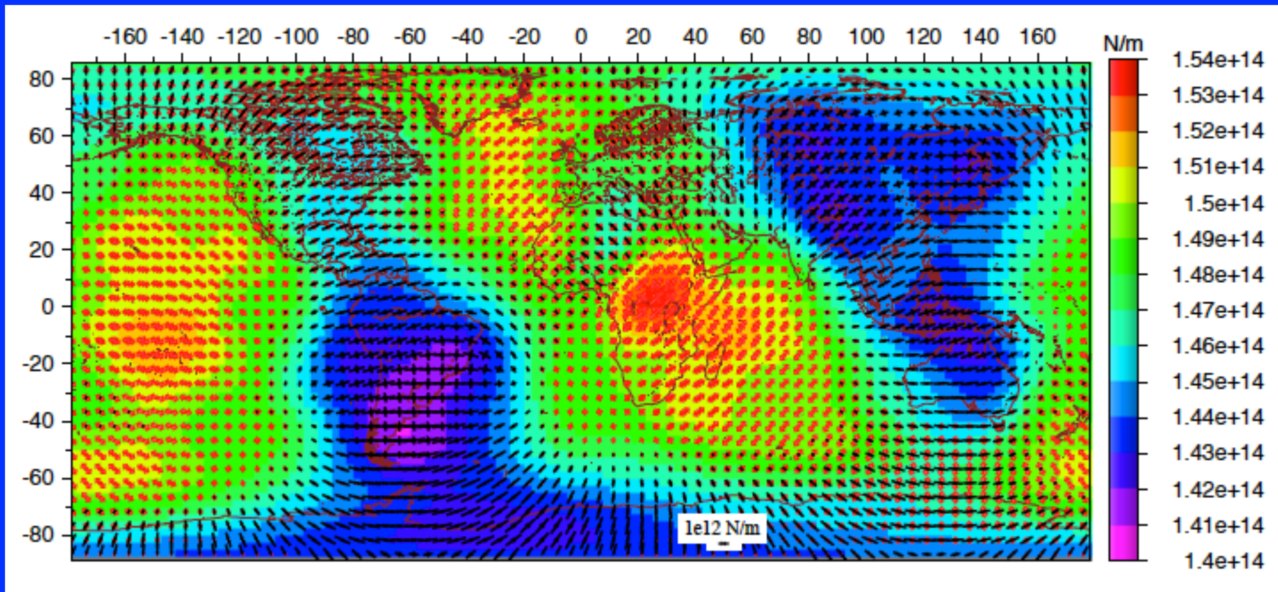

Ghosh et al. [2008], **GRL**

Thin Sheet deviatoric stress response to GPE differences, created by dynamic Topography, created in 3-D global convection model

Benchmarking with 3-D spherical convection

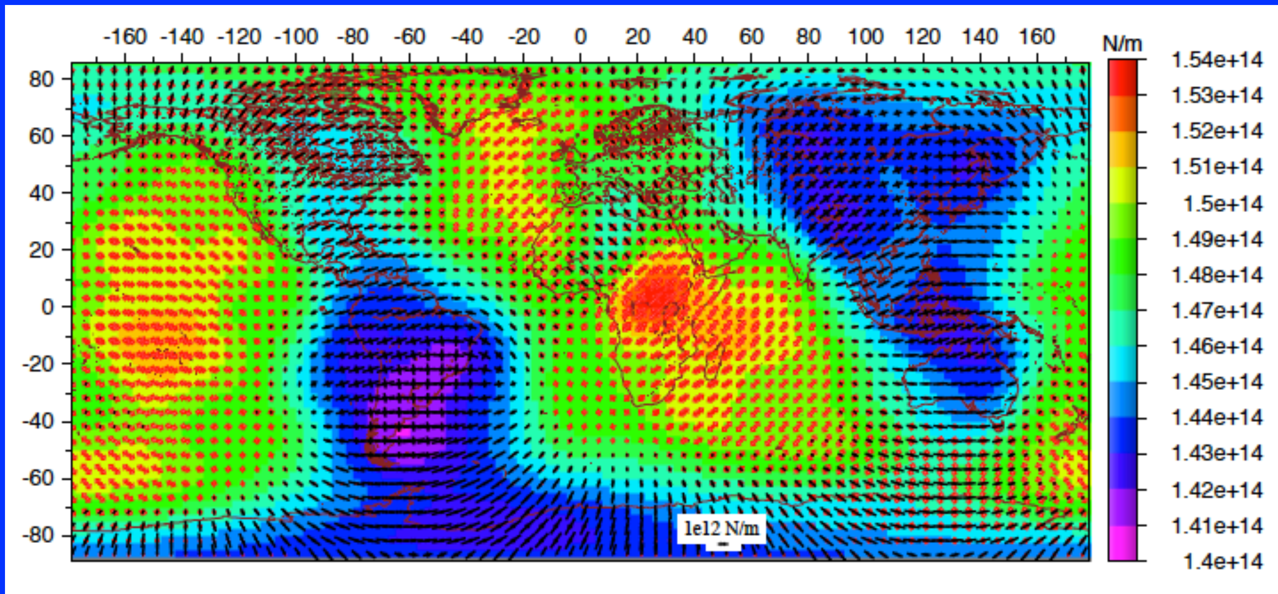

Ghosh et al. [2008], **GRL**

Thin Sheet deviatoric stress response to GPE differences, created by dynamic Topography

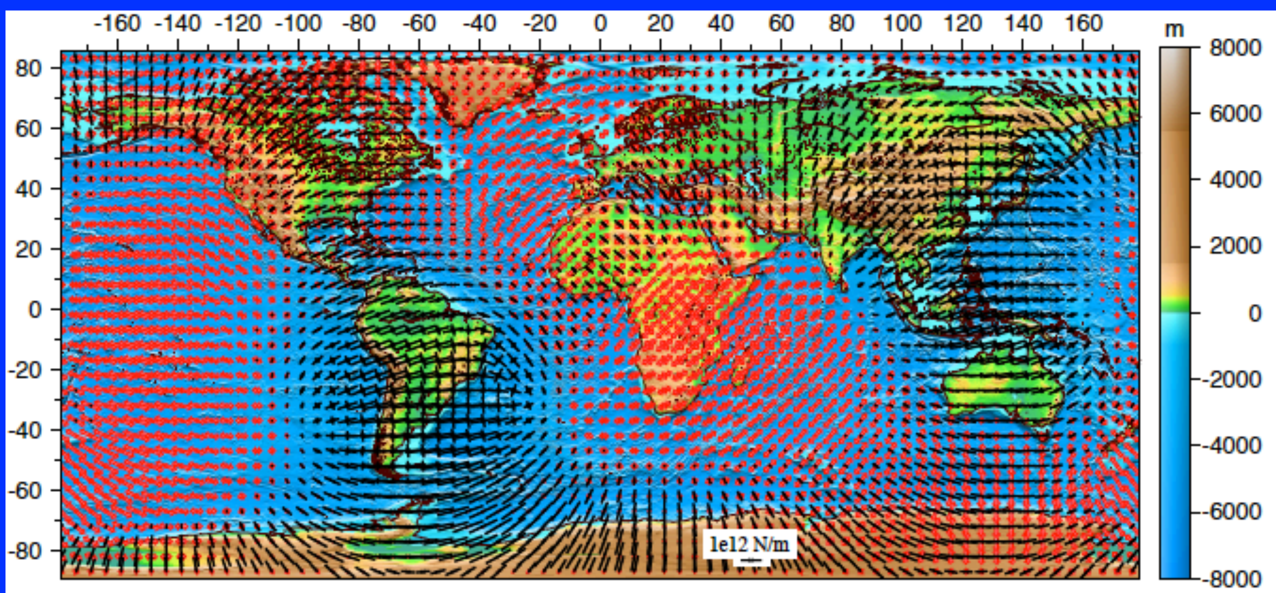

Thin sheet deviatoric stress response to tractions applied at base

Comparison of thin sheet stresses with output from full 3-D model

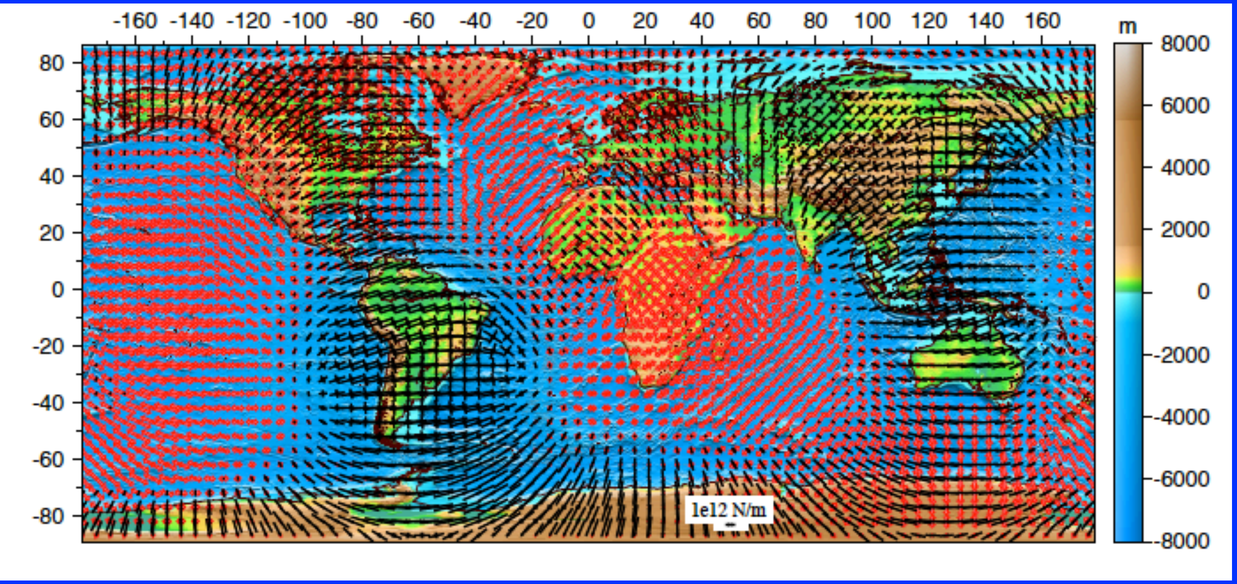

Total thin sheet response = traction solution + GPE solution (lithosphere finite element solution)

Ghosh et al. [2008], **GRL**

Comparison of thin sheet stresses with output from full 3-D model

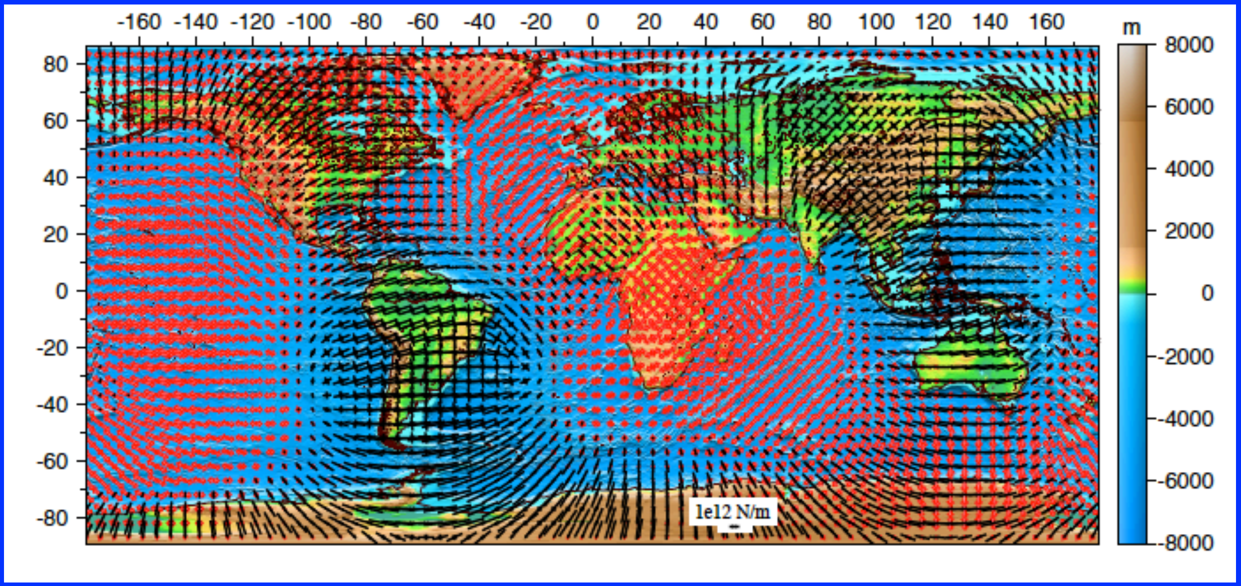

Total thin sheet response = traction solution + GPE solution (lithosphere finite element solution)

Ghosh et al. [2008], **GRL**

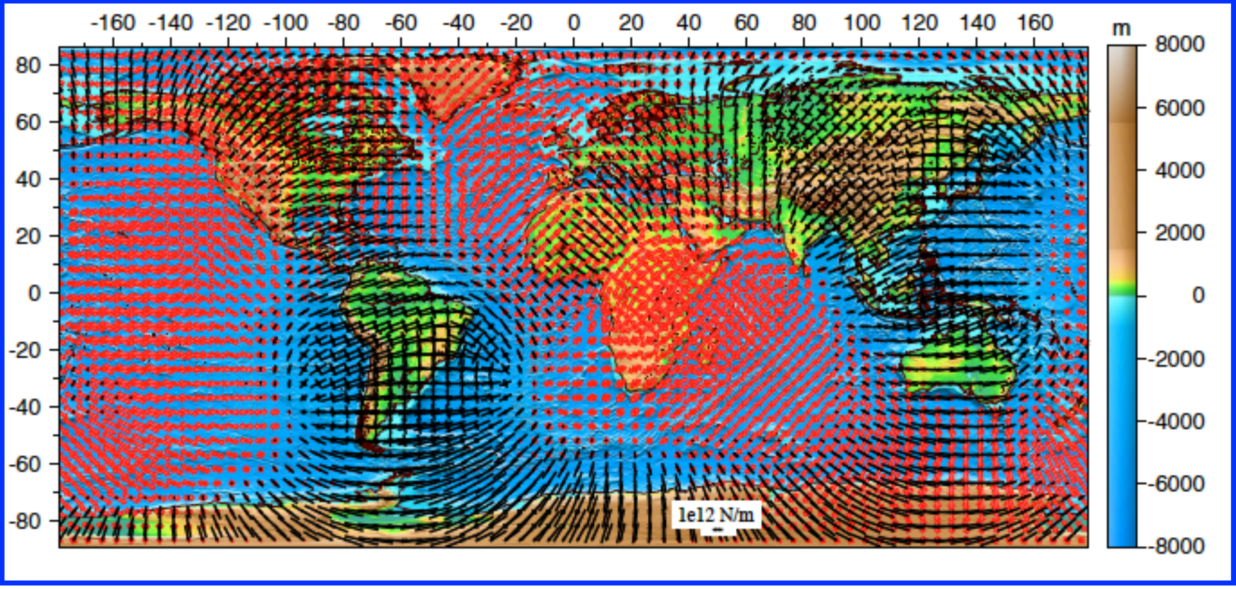

Deviatoric Stress output from the full 3-D convection model

Agreement in magnitude

Agreement in orientation and style

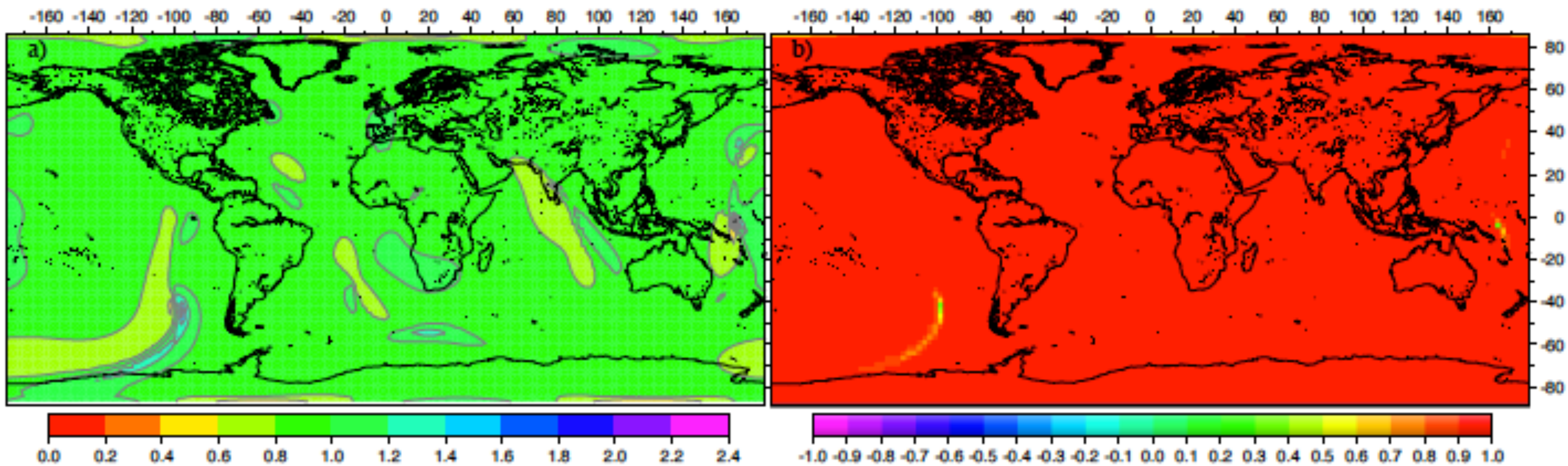

$(T_{\text{thin sheet}})/(T_{3\text{-}D})$

Ghosh et al. [2008], **GRL** (see suppl.)

*Variable viscosity case benchmarked by *Klein et al*. [2009], JGR

Correlation between tensor field from thin sheet with tensor field from global 3-D model = $\tau_1 \bullet \tau_2 / T_1 T_2$

Summary from benchmarking

- Can recover the deviatoric stress field given accurate estimates of (1) topography, crustal and upper mantle structure, and (2) knowledge of applied horizontal tractions from mantle flow (reliable convection models).
- If you know surface motions, then you can also recover the absolute values of effective viscosity

Benchmarking with lateral viscosity variations

- lateral viscosity variations of 2 order magnitude in full 3-D convection model

- An approximation of the relative viscosity variations (but not exact) was used in the thin sheet model
- Stresses were recovered in thin sheet model with the worst misfits in magnitudes off by factor of 2 in areas with significant lateral variation in viscosity

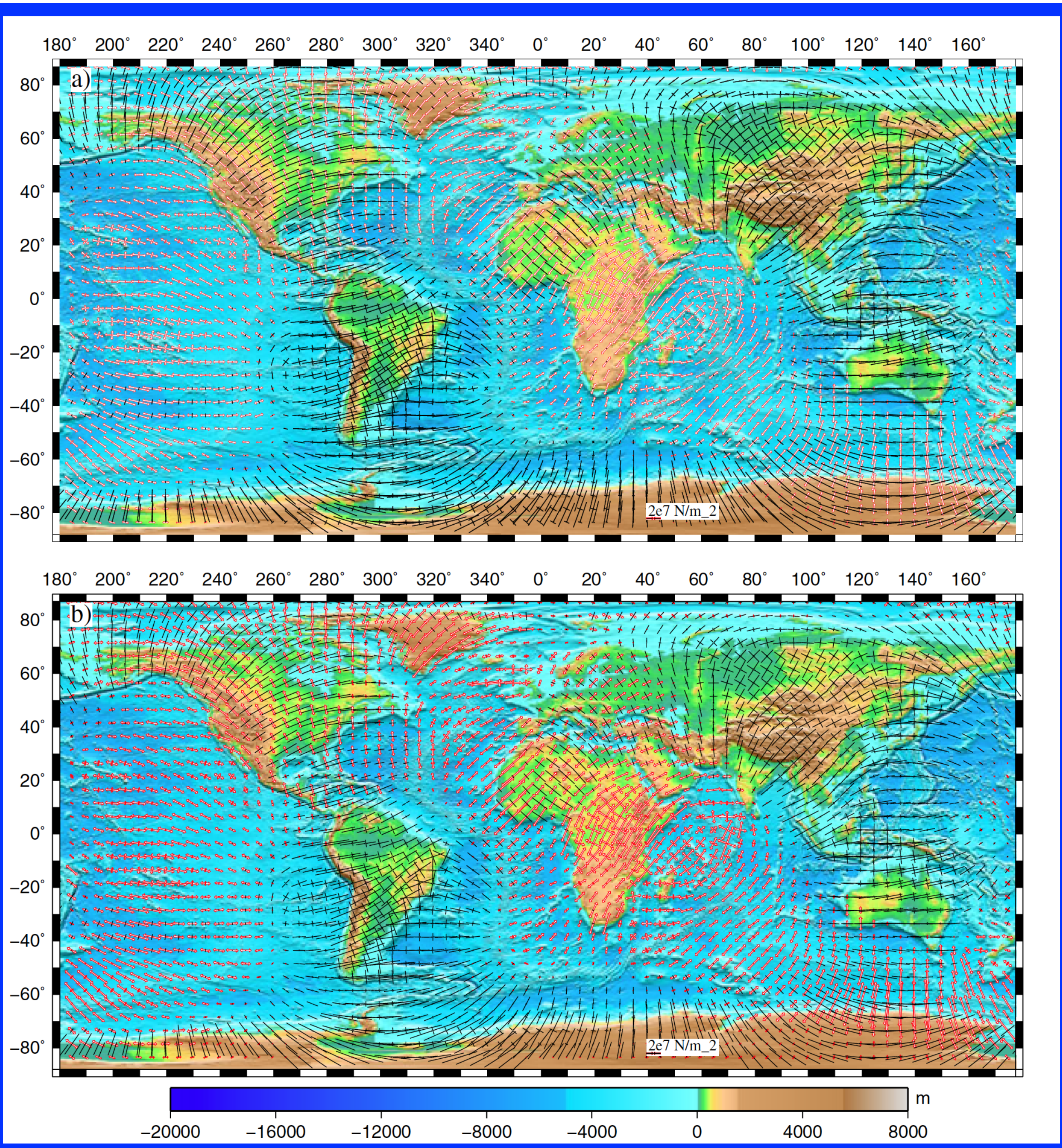

Thin sheet output = dynamic topo + traction contributions + using relative viscosity variations

Output from full 3-D global model with lateral viscosity variations

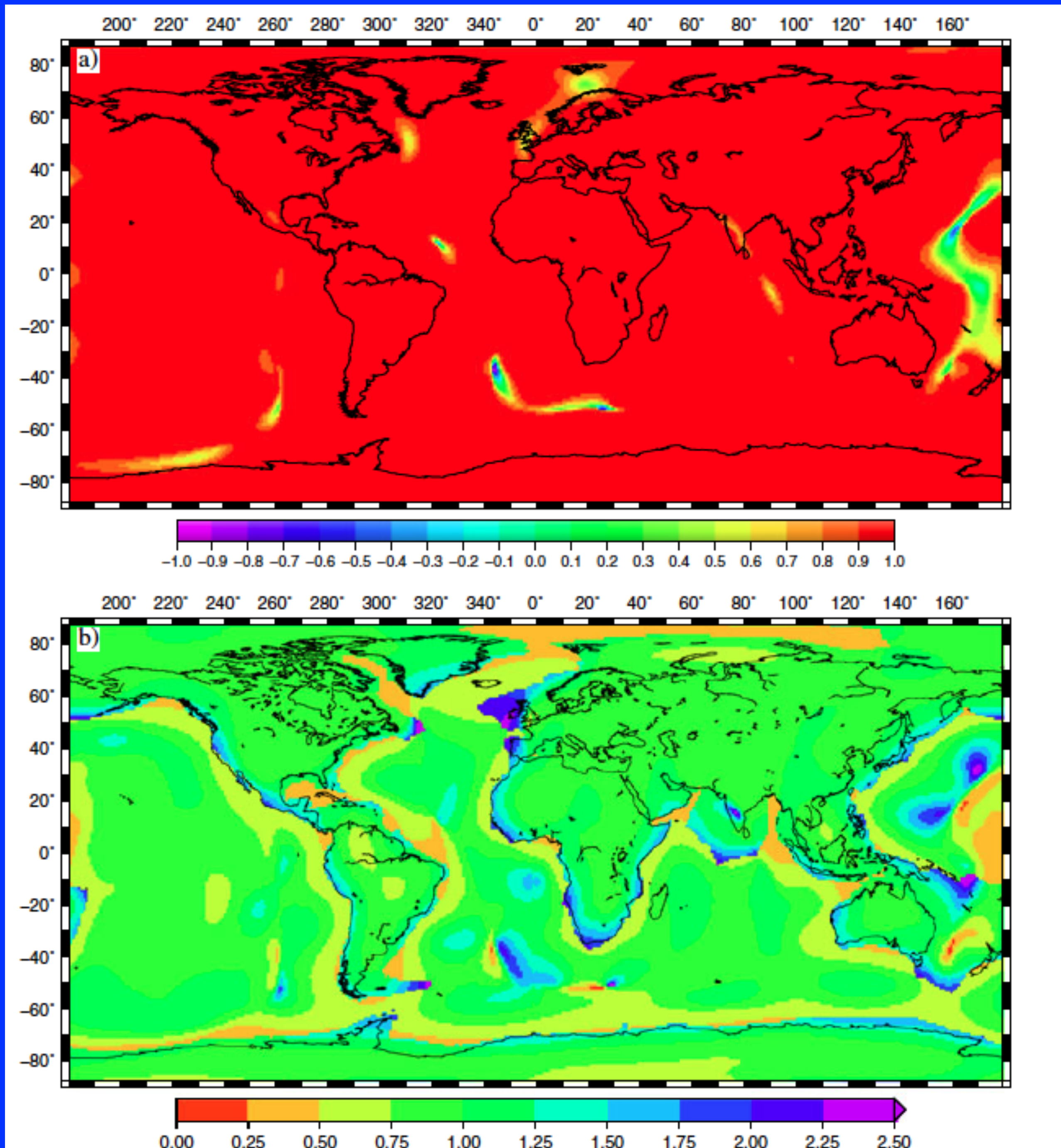

Correlation between tensor field from thin sheet with tensor field from global 3-D model $= \tau_1 \bullet \tau_2 / T_1 T_2$

$(T_{\text{thin sheet}})/(T_{\text{3-D}})$

Forward Dynamic Modeling: Adjustable Parameters

- Lateral viscosity structure of lithosphere
  - Location of keels, cratons, and plates
  - Old vs. Young Ocean lithosphere
  - Location of plate boundary zones and their viscosity distribution

- Mantle Radial Viscosity Profile

Global Modeling to Compute Stresses, Strain Rates, and Surface Motions: (1°x1° grid with over 63,000 elements)

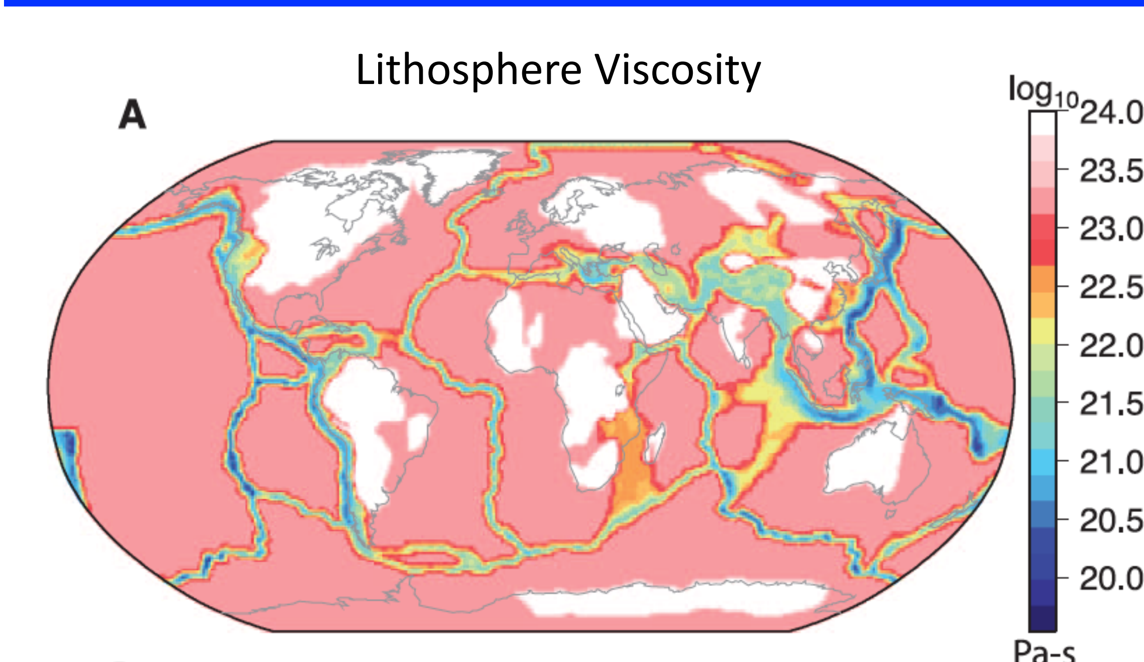

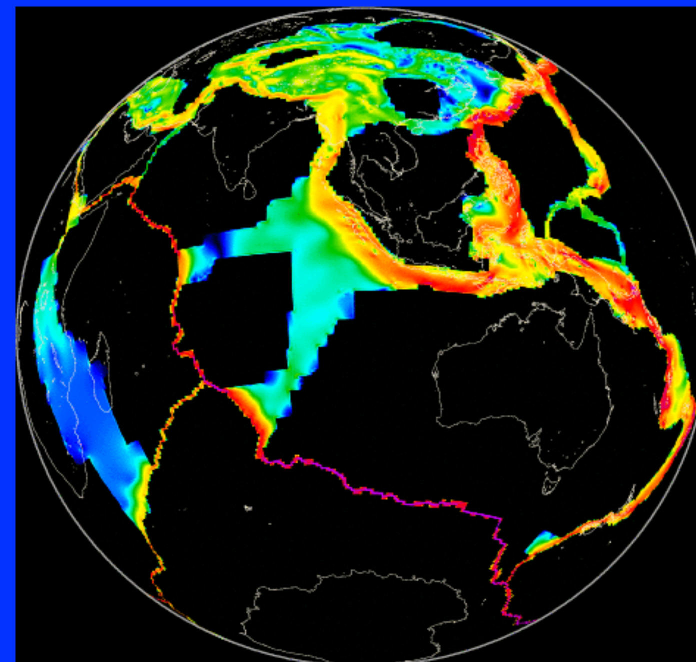

Ghosh and Holt, 2012 *Science*

Relative viscosity variation:

$$\frac{1}{\mu} = 1 + \left(\frac{1}{\mu_{ref}} - 1\right)\sqrt{\frac{E^2}{E_{ref}^2}}$$

Plates = 1

Cratons = 10

E = scalar second invariant of strain rate from GSRM [Kreemer et al., 2003]

E_{ref} = E value corresponding to area with μ_{ref}

μ_{ref} = viscosity for area with E_{ref}

Global Modeling to Compute Stresses, Strain Rates, and Surface Motions

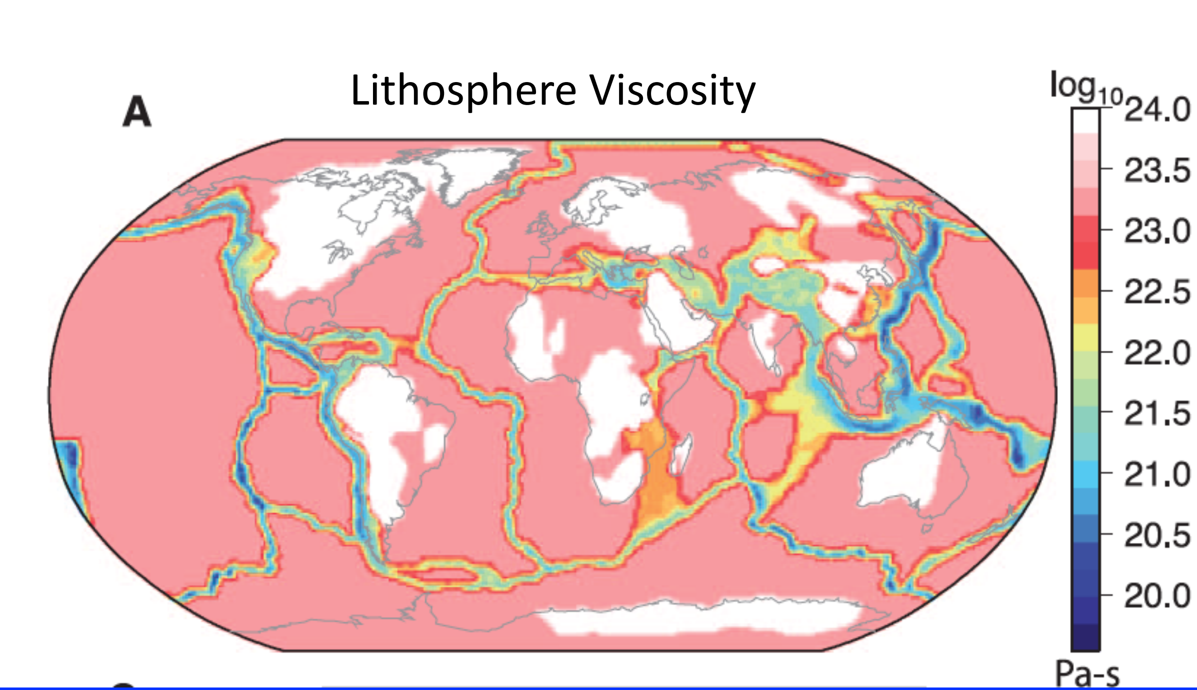

Ghosh and Holt, 2012 *Science*

$$\frac{1}{\mu} = 1 + \left(\frac{1}{\mu_{ref}} - 1\right)\sqrt{\frac{E^2}{E_{ref}^2}}$$

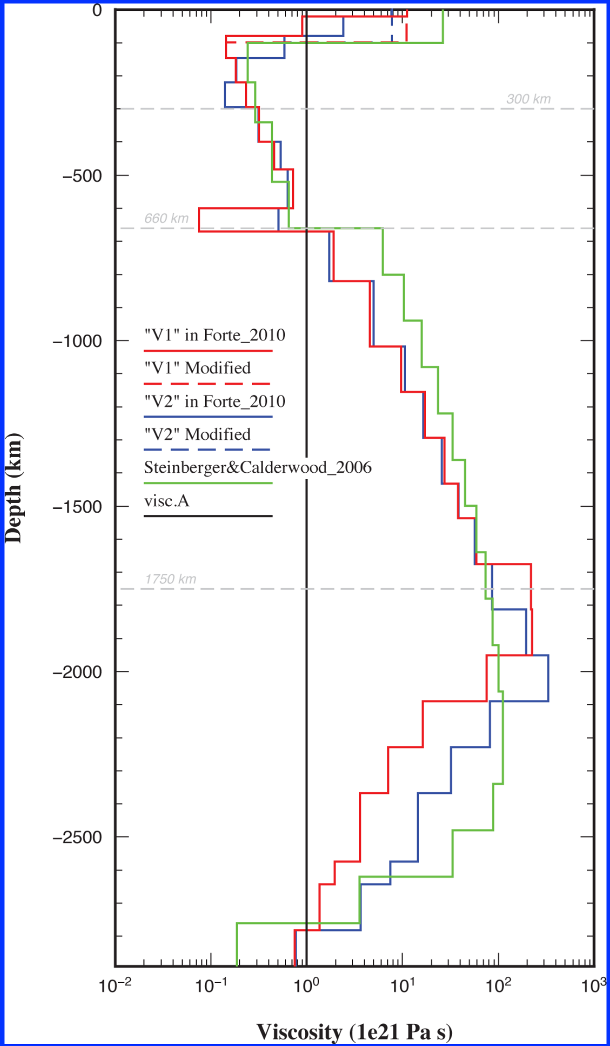

Radial Viscosity Profiles

For E_{ref}= 3e-7/yr we tried μ_{ref}=1/10; 1/30; 1/100; 1/1000

Results from 300 forward models

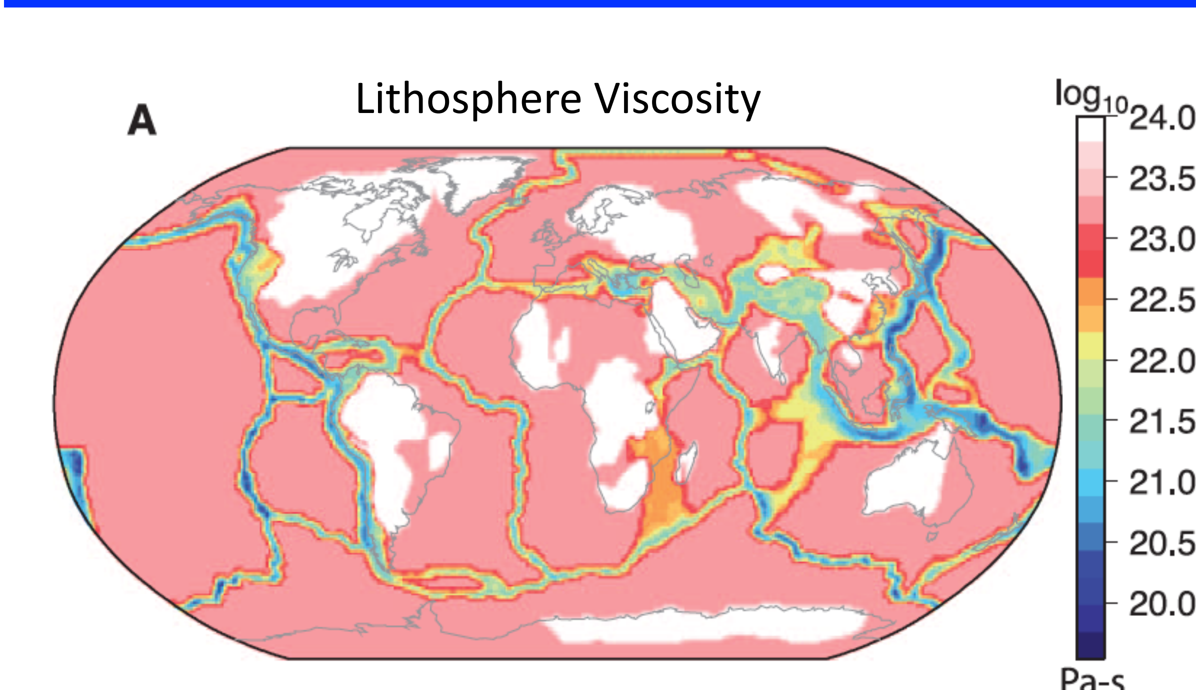

Ghosh and Holt, 2012 *Science*

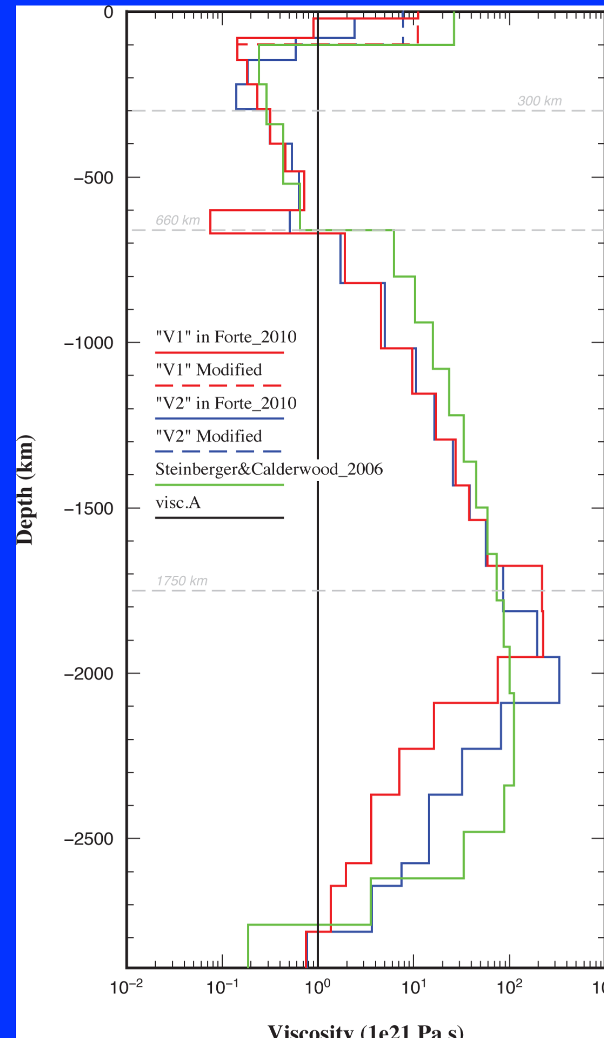

Radial Viscosity Profiles

Plates = 1e23 Pa-s
Cratons = 1e24 Pa-s
Deeper Continental Keels = 1e21 – 1e22 Pa-s
Asthenosphere = 1e20 Pa-s
Plate Boundary Zones = Variable Viscosity
Variety of published tomography models have been tried

Stresses from Topography and Lithosphere Structure

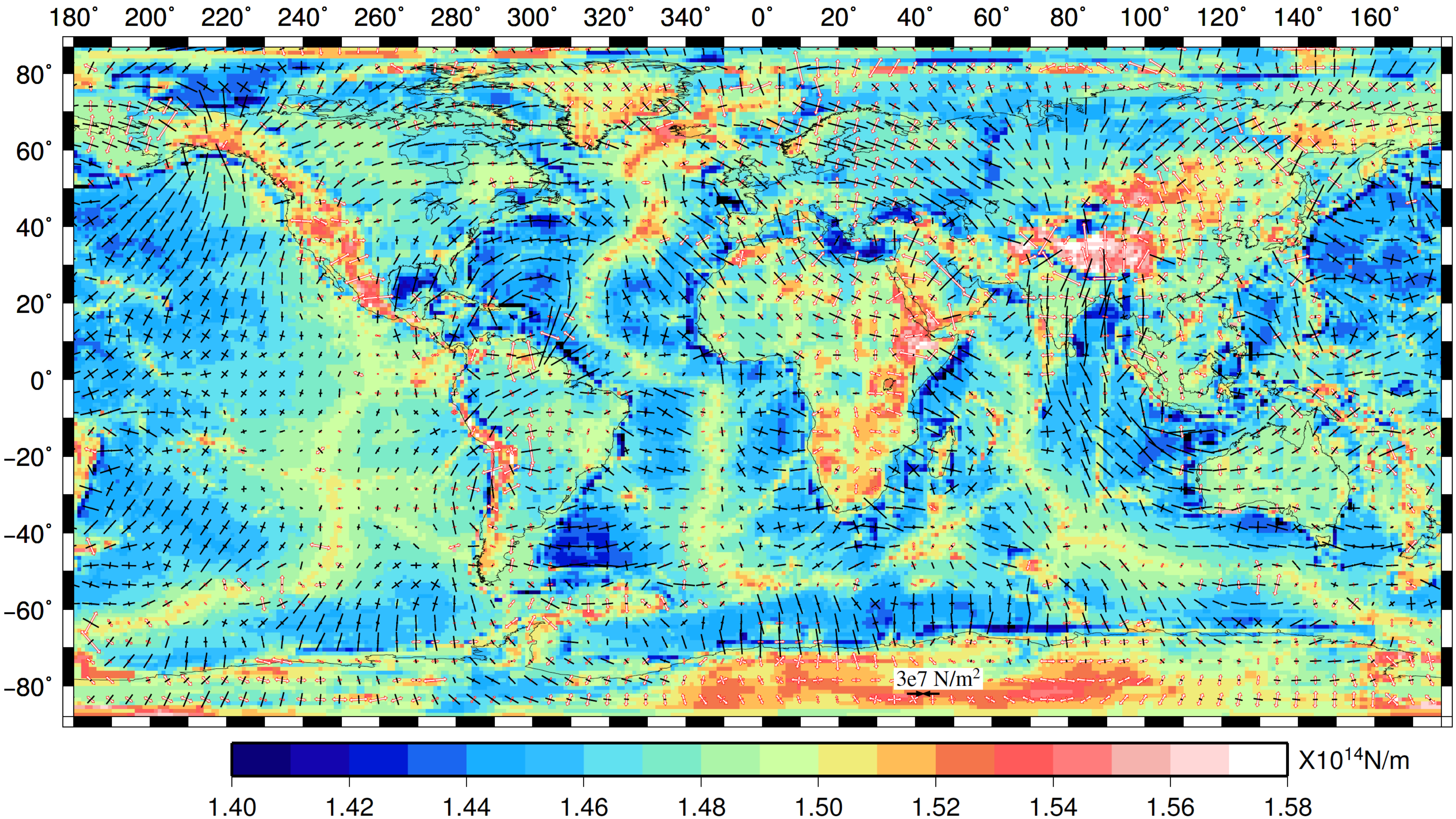

Ghosh, Holt, Wen, 2013, JGR

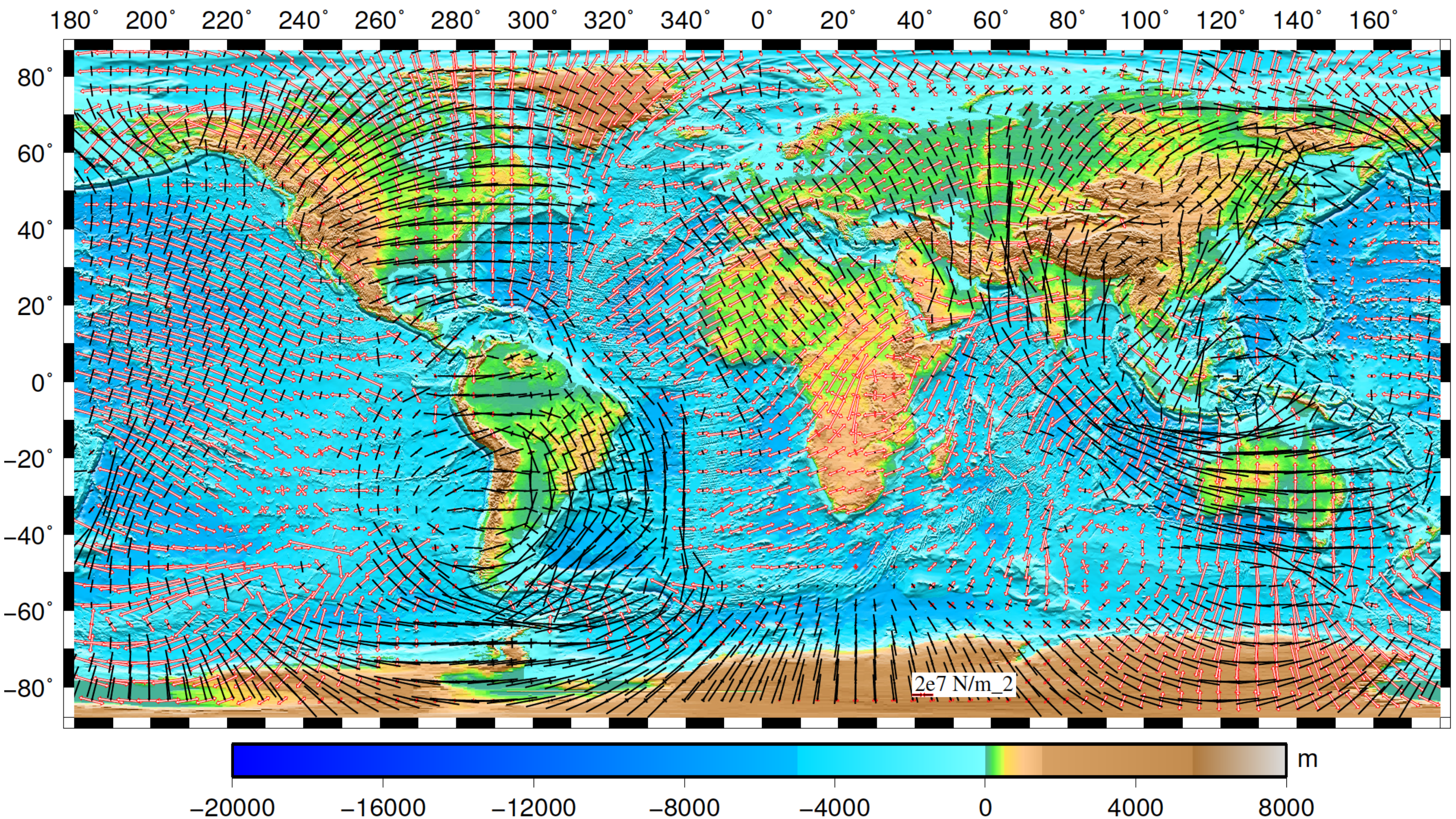

Dev. Stress from tractions associated with mantle flow

Ghosh et al. [2013] *J.G.R*

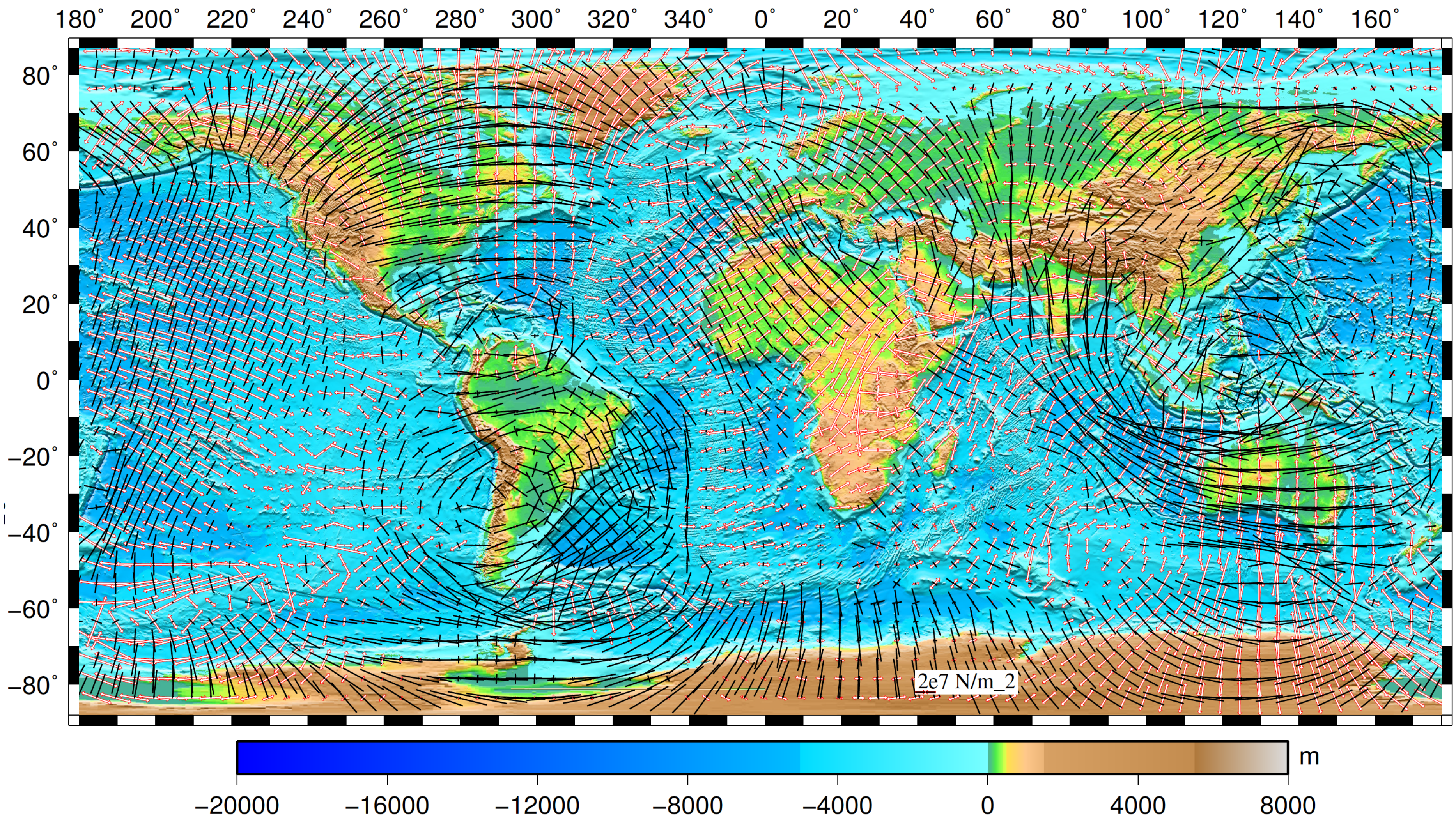

Total Dev. Stress from GPE + tractions *Ghosh et al*. [2013] *J.G.R*

Compare with WSM in plates and GSRM in plate boundary zones

Results: Plate Motions

Mantle tractions

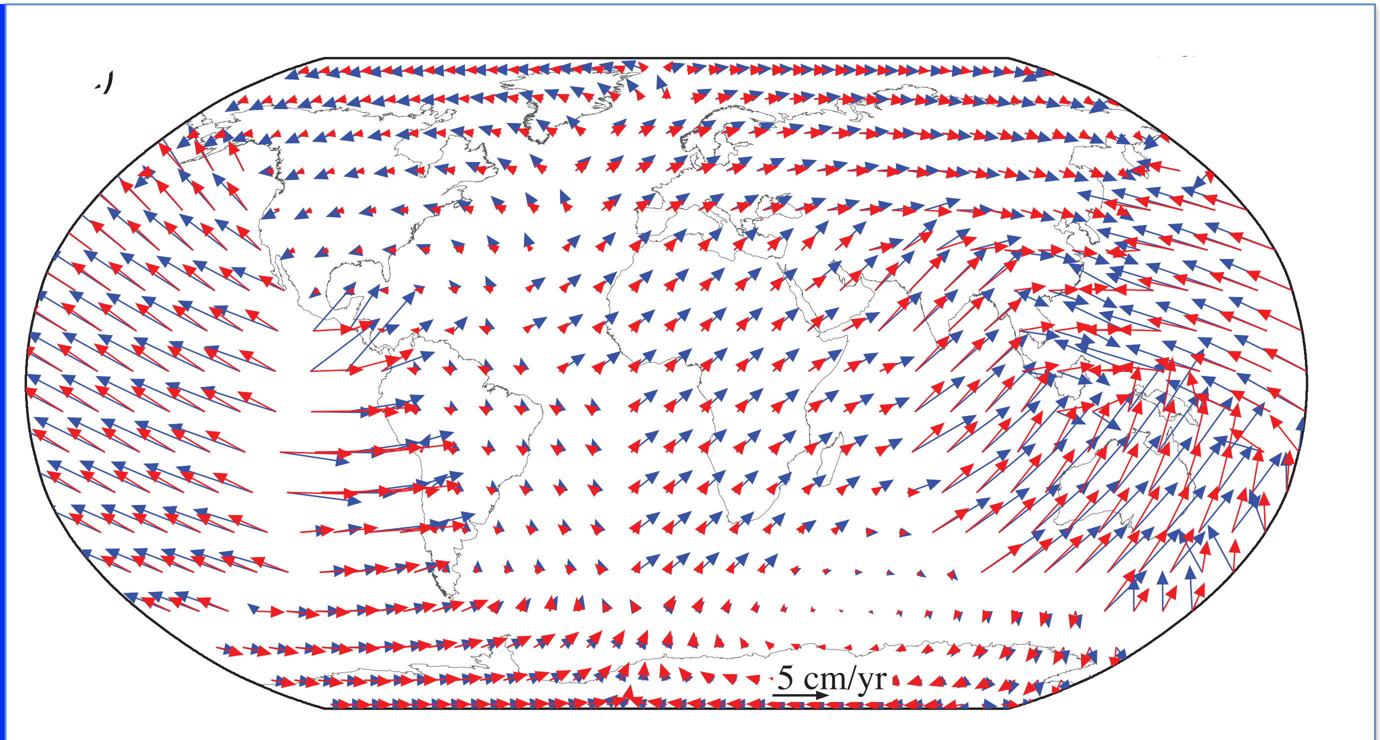

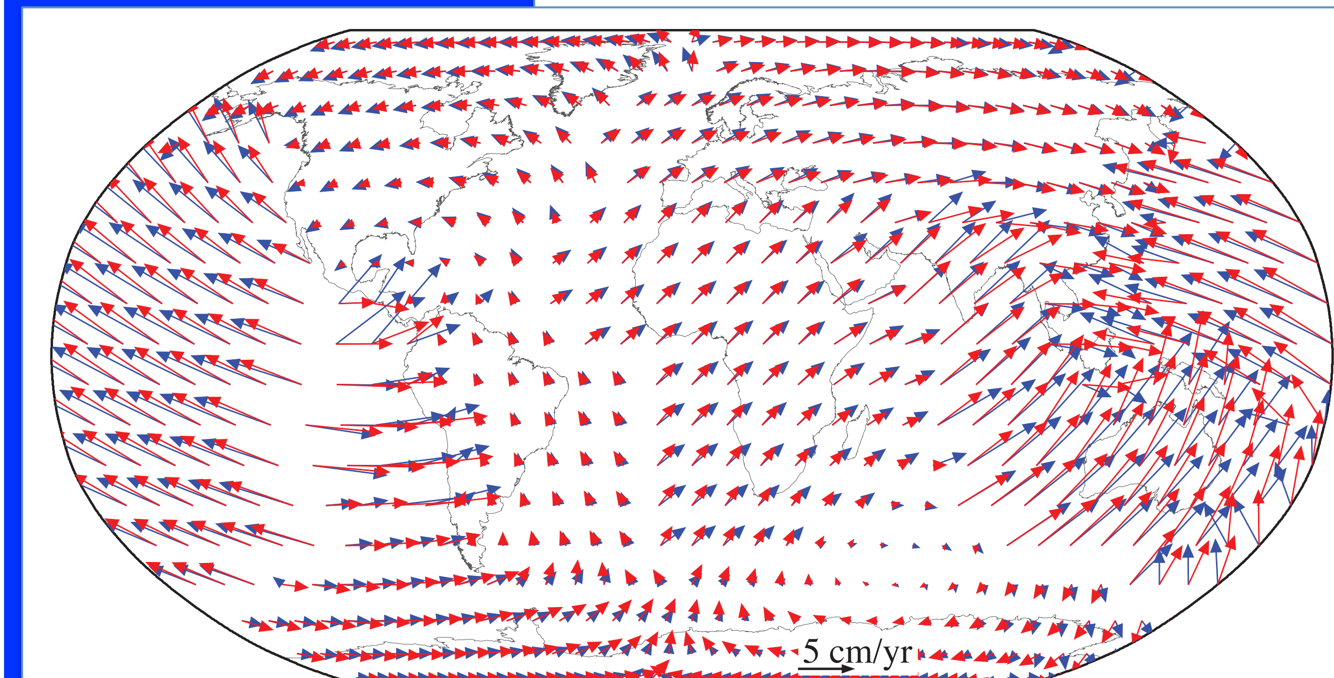

Mantle tractions + GPE

Ghosh and Holt, Science (2012)

RMS misfit < 1 cm/yr

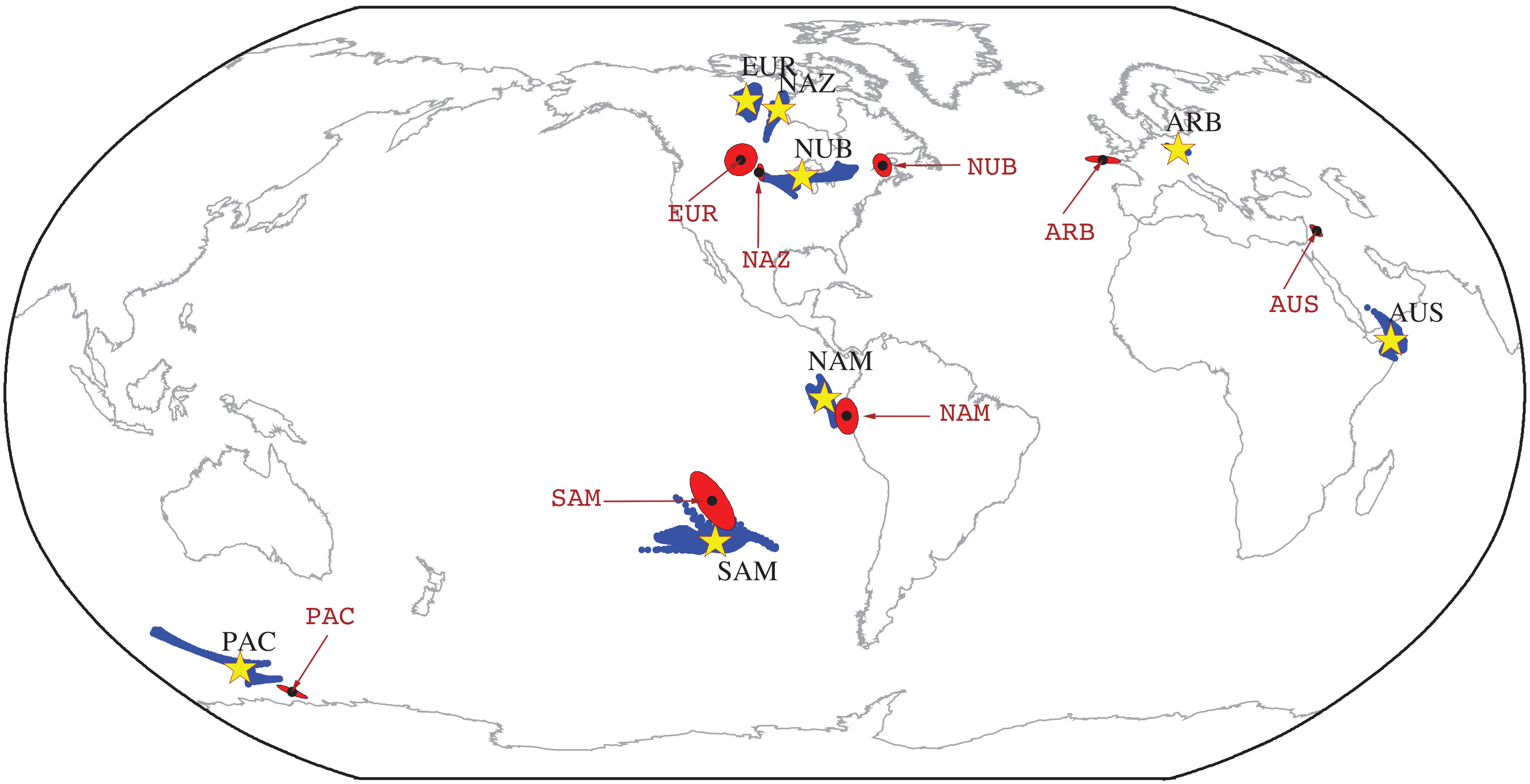

Poles of rotation from dynamic model compared with DeMets et al. [2011]

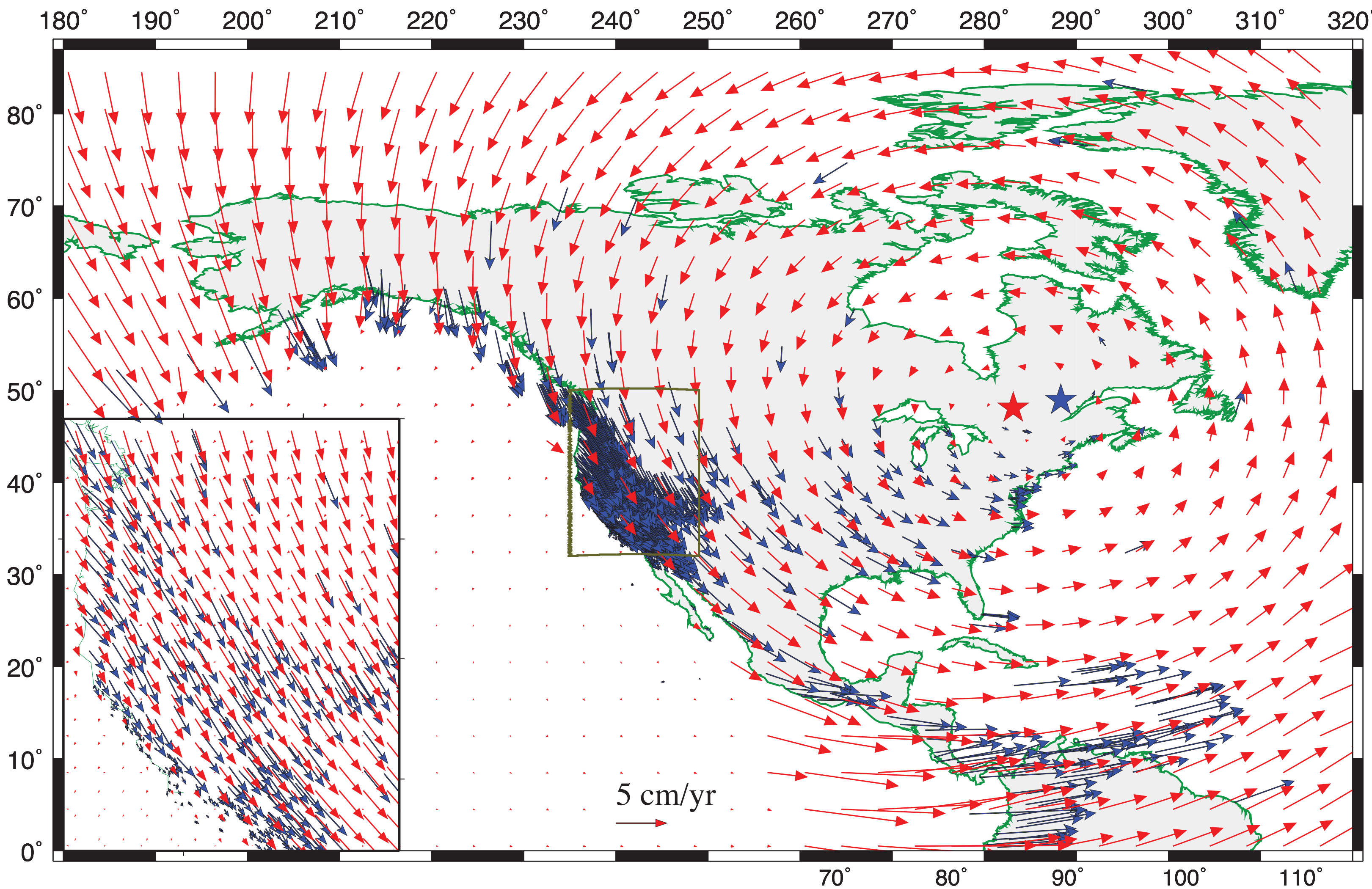

180˚
190˚
200˚
210˚
220˚
230˚
240˚
250˚
260˚
270˚
280˚
290˚
300˚
310˚
320˚
80˚
70˚
60˚
50˚
40˚
30˚
20˚
10˚
0˚
5 cm/yr
70˚
80˚
90˚
100˚
110˚

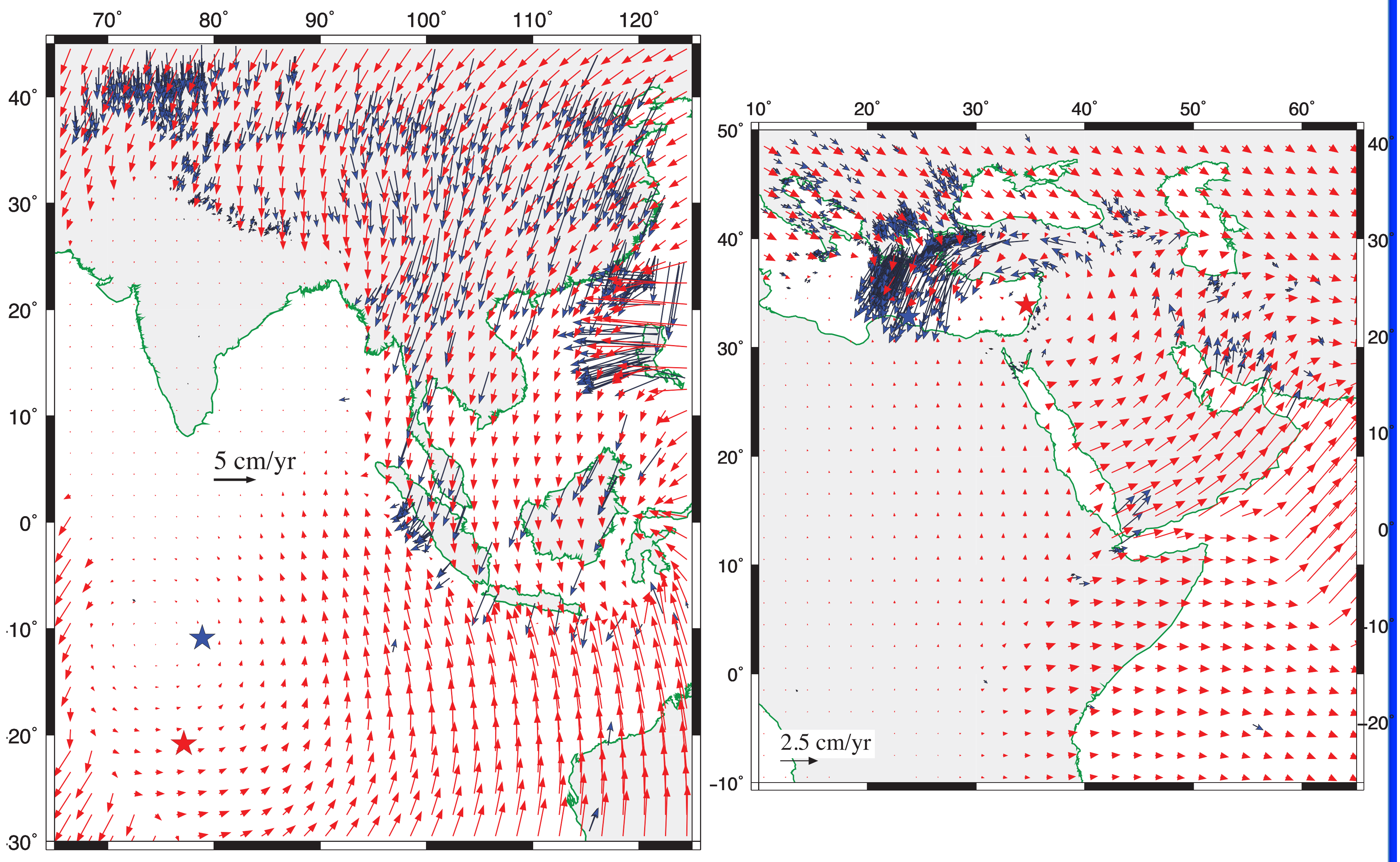

Ghosh and Holt, (2012)

Results: Deviatoric Stresses

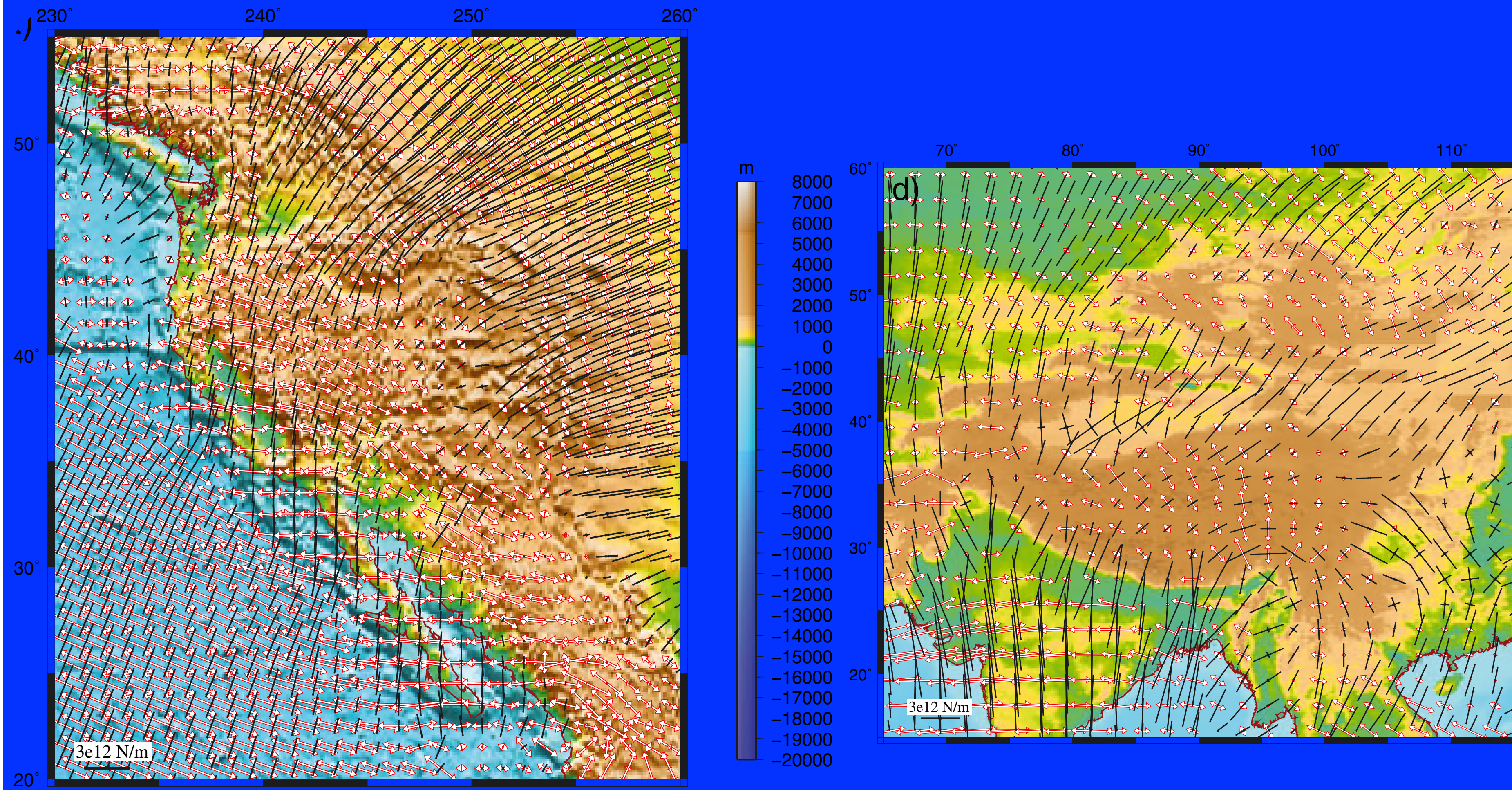

Ghosh et al., JGR (2013)

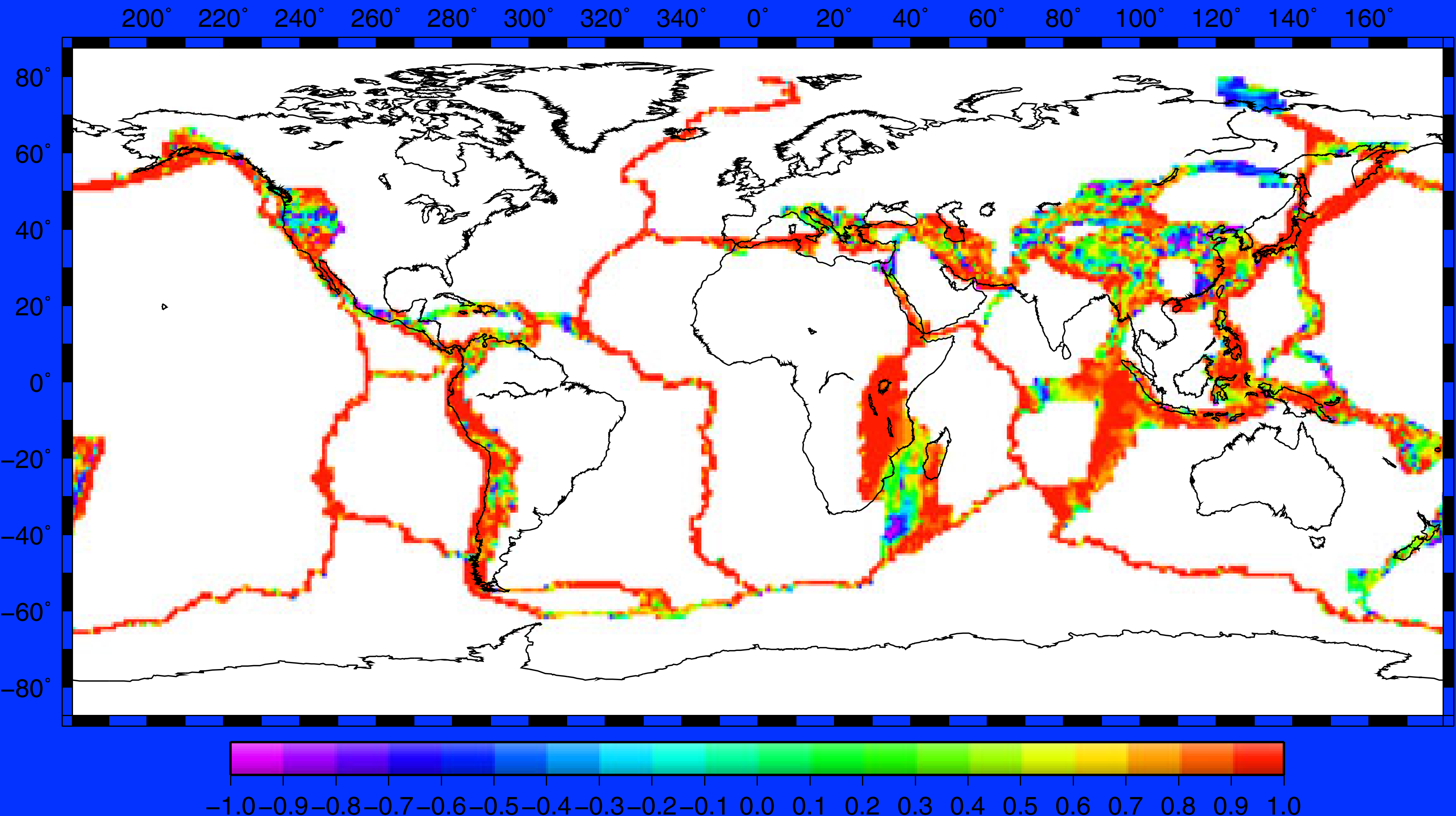

Correlation between predicted deviatoric stresses and strain rates from GSRM

Ghosh et al., JGR (2013)

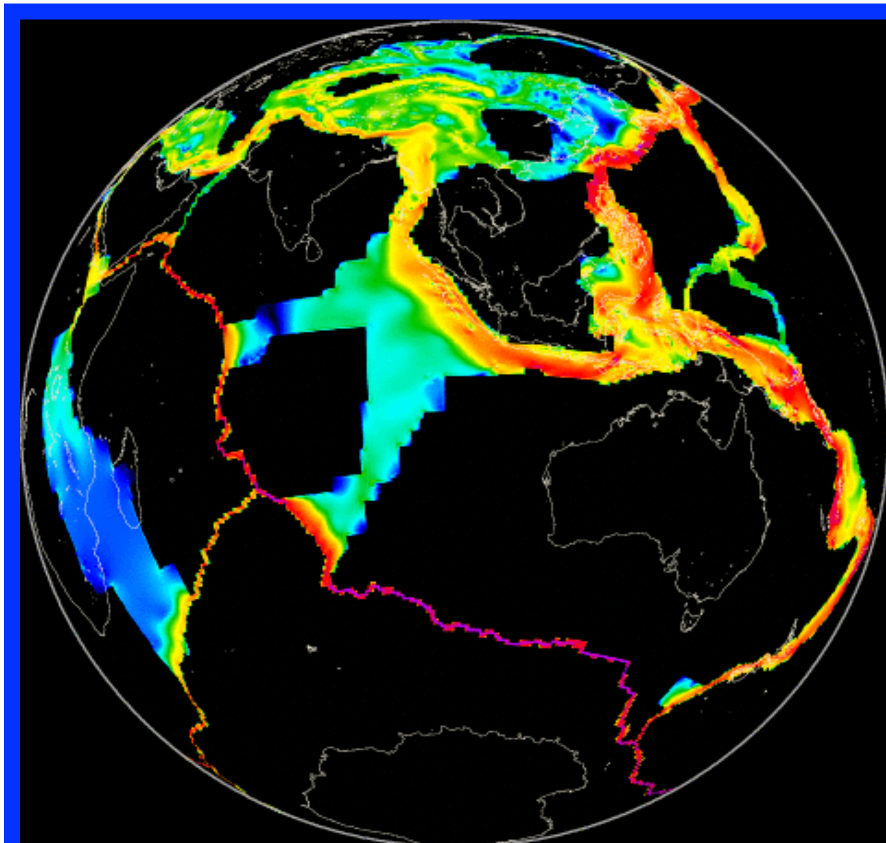

Global Strain Rate Model

(*Kreemer et al., 2003*)

- Direction of principal axes
- Fault style

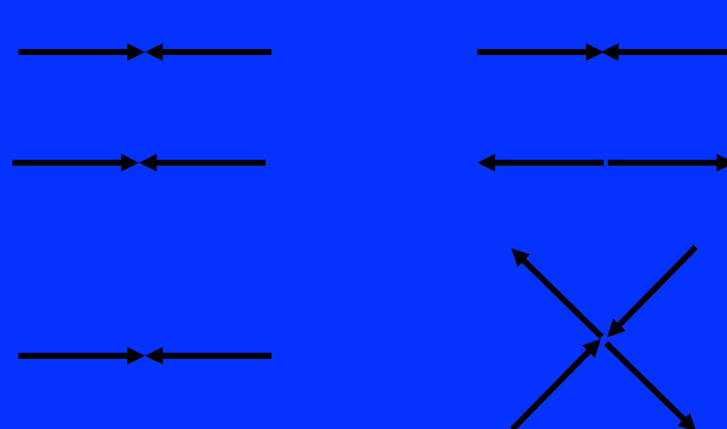

Correlation coefficient

$$-1 \le \sum_{areas} (\varepsilon \cdot \tau)\Delta S \Big/ \left(\sqrt{\sum_{areas} (E^2)\Delta S} * \sqrt{\sum_{areas} (T^2)\Delta S} \right) \le 1$$

Region of Interest	Number of Areas	GPE	Tractions	Differences Plus Basal Tractions
Western North America	618	0.46	0.81	0.78
Andes	440	–0.16	0.98	0.93
Eastern Africa	865	0.32	0.91	0.87
Mediterranean	352	0.68	0.59	0.75
Central Asia	995	0.25	0.62	0.61
Indo-Australian plate boundary zone	836	0.84	0.84	0.90
Mid-oceanic ridges	916	0.94	0.96	0.97
Western Pacific	538	0.42	0.87	0.84
Southeast Asia	800	0.59	0.77	0.82
Total	8588	0.60	0.84	0.85

Comparison with World Stress Map

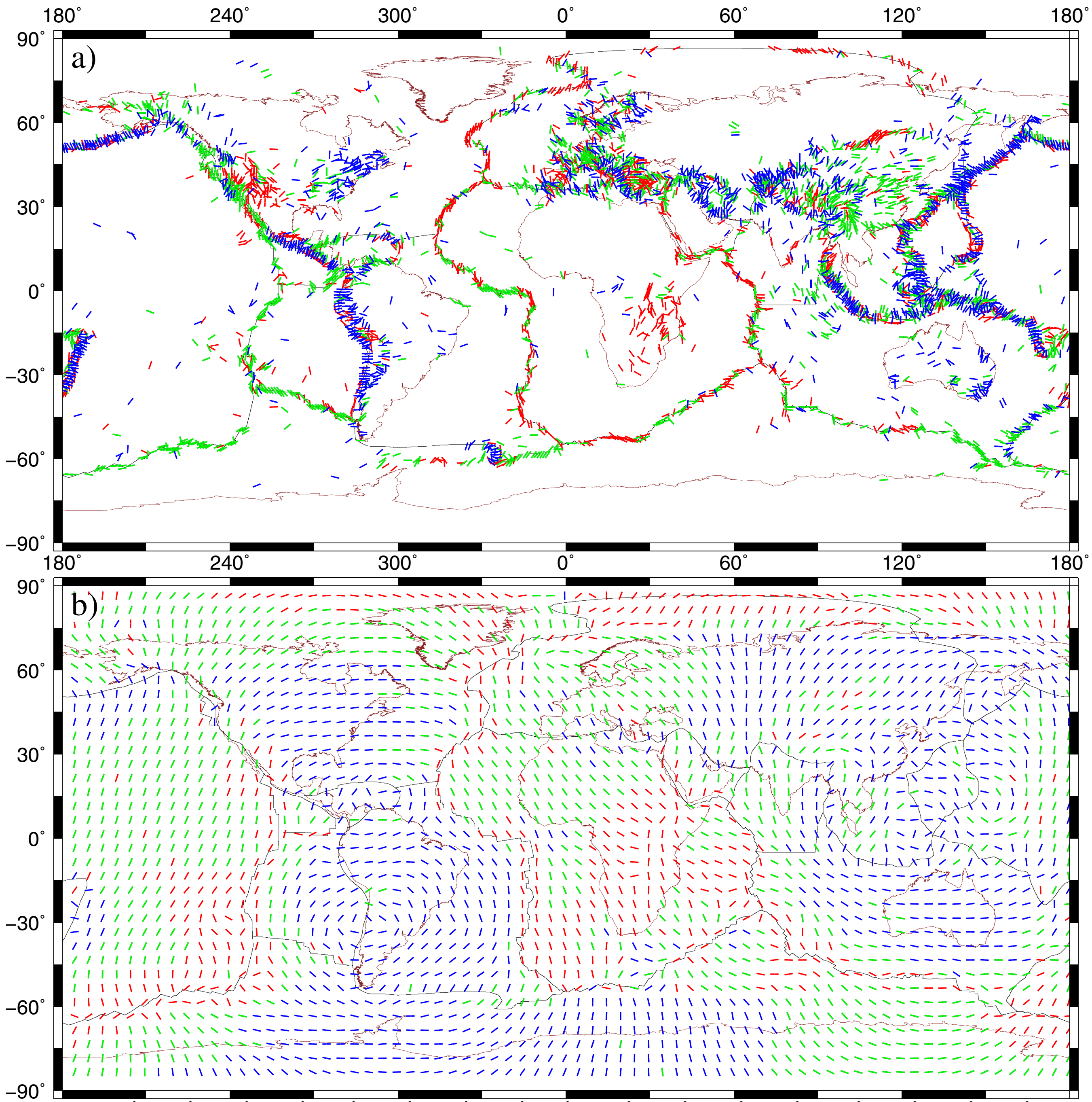

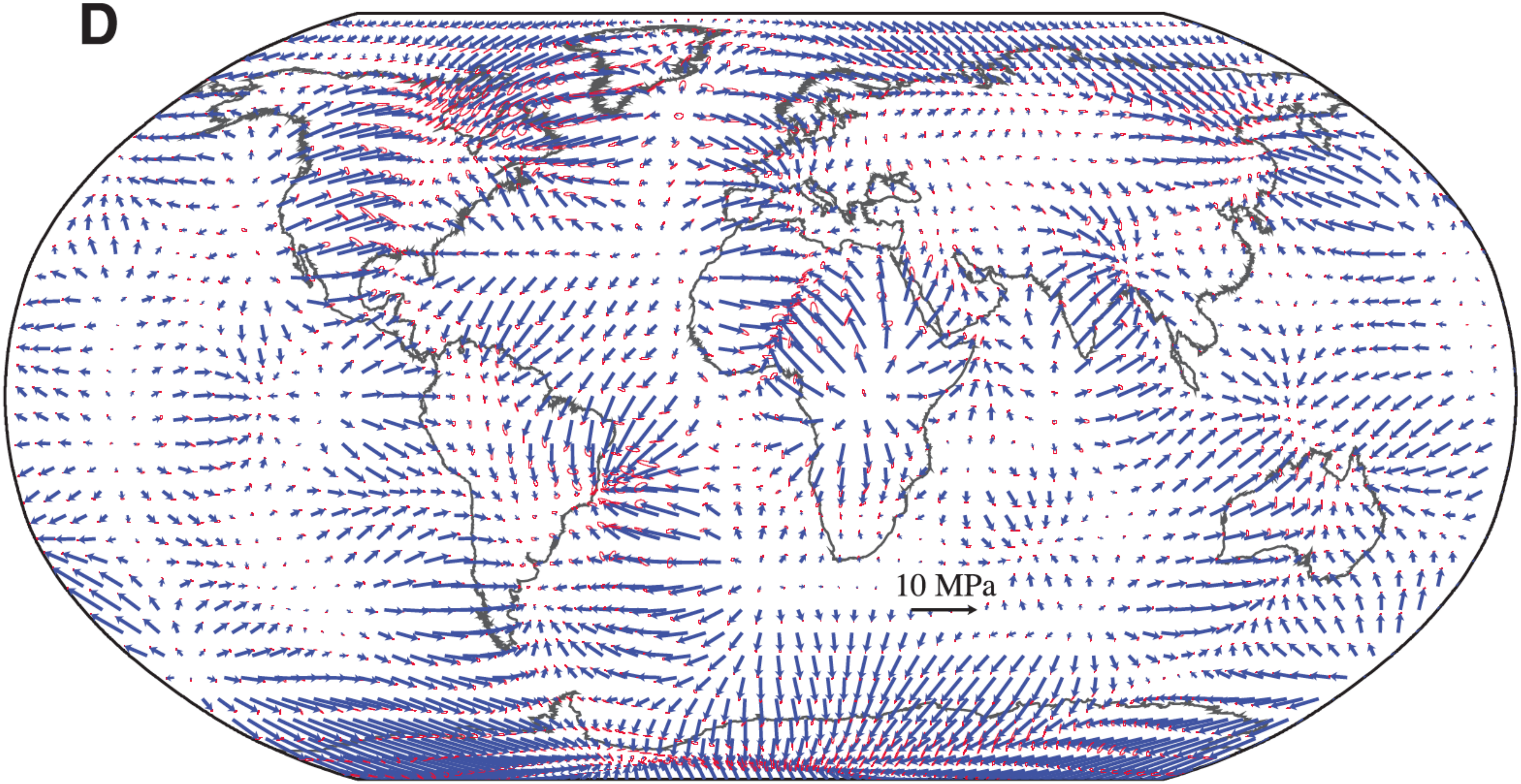

Tractions at base of lithosphere imposed by mantle flow
Ghosh and Holt [2012] *Science*

Second Invariant of Deviatoric Stresses

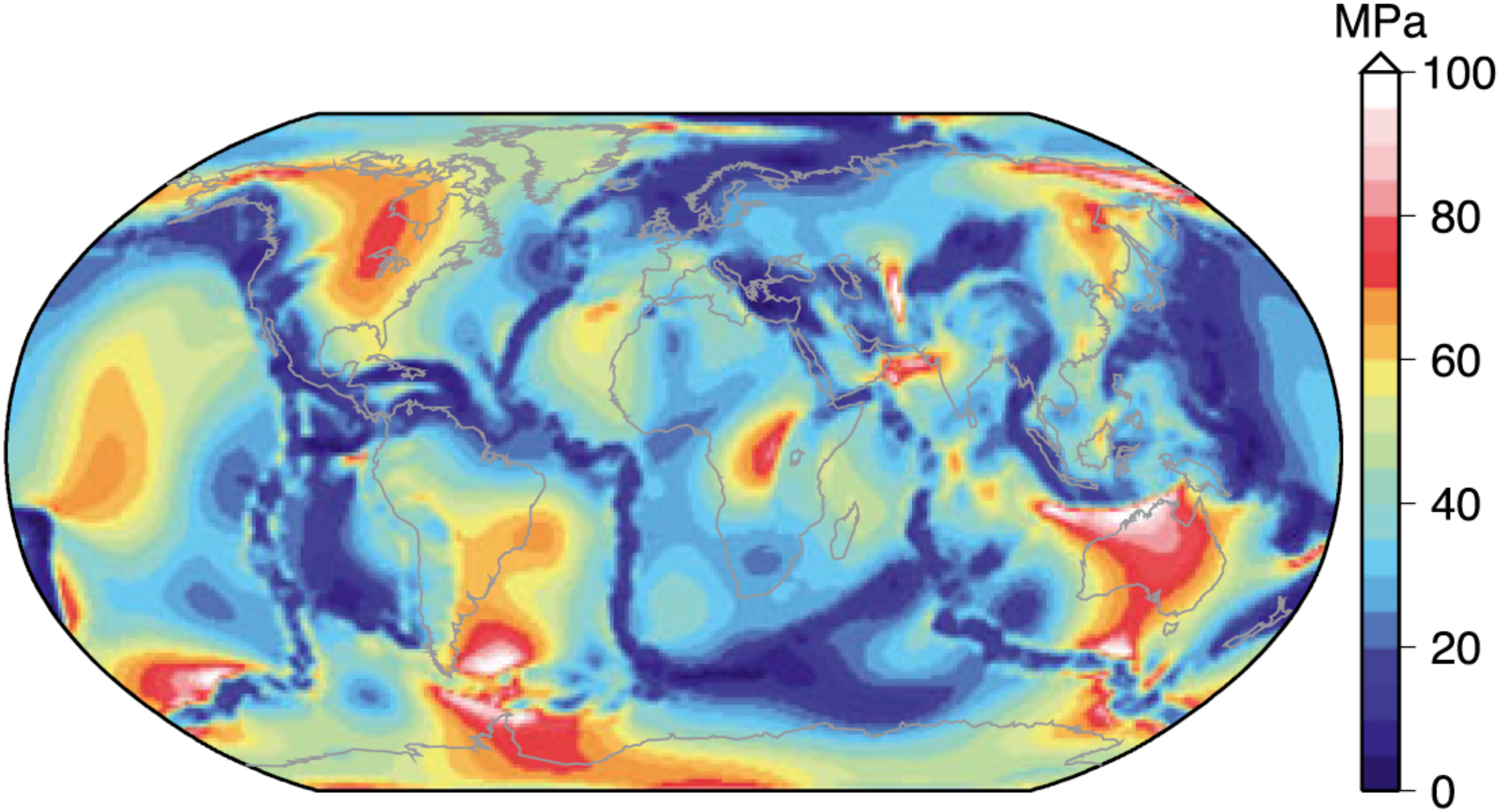

Strain Rates

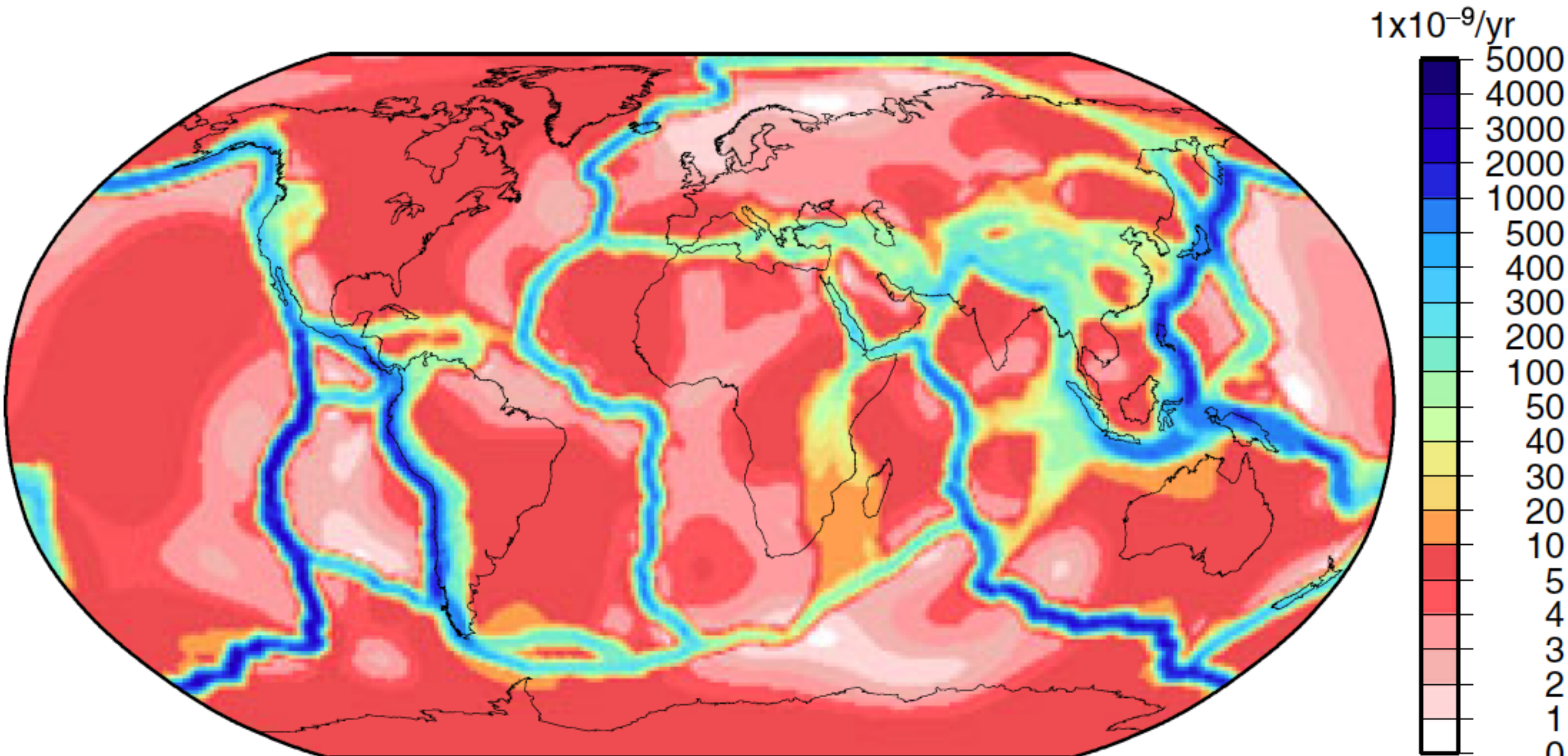

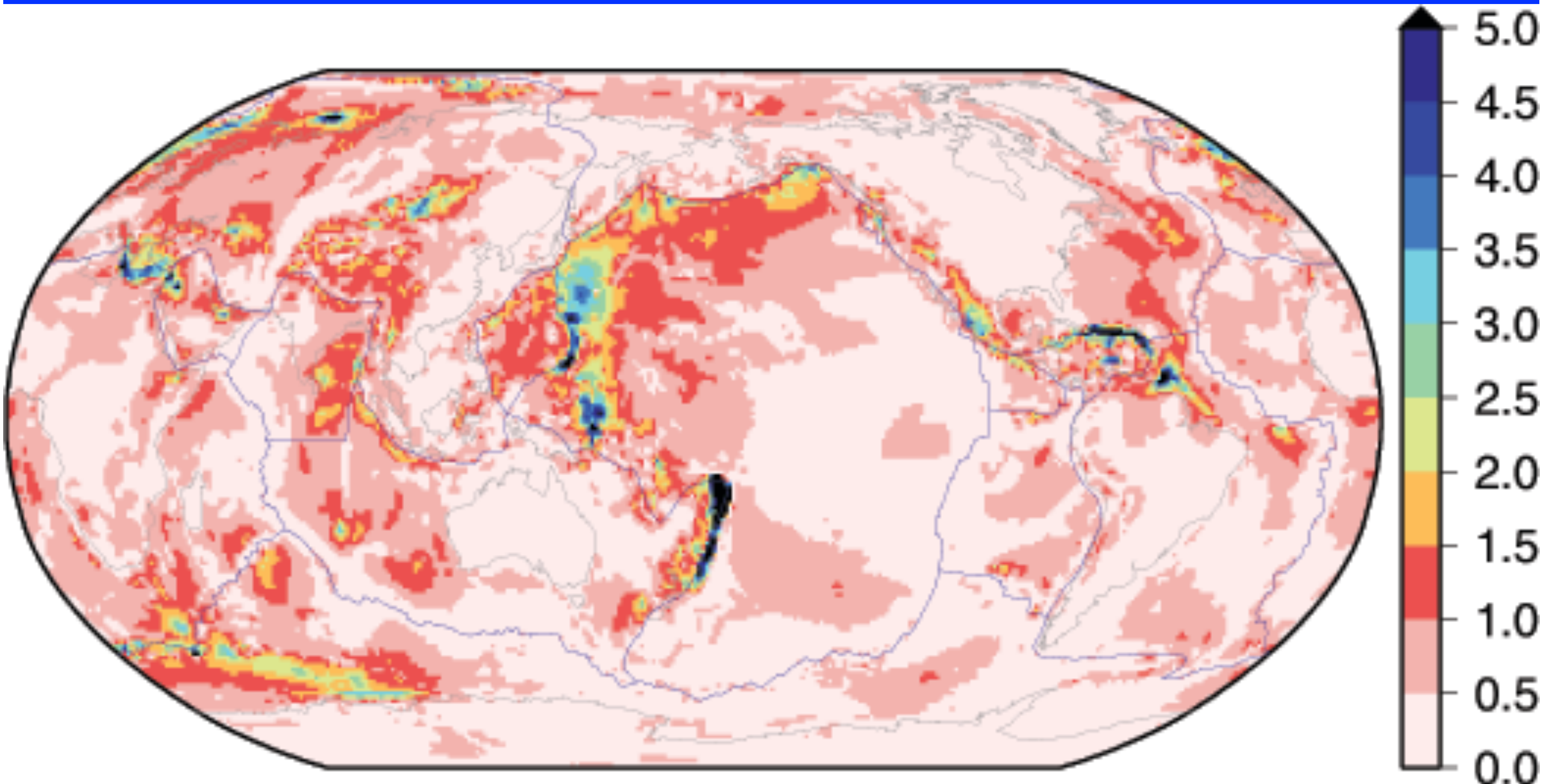

T(GPE)/T(Tractions)

Tractions from mantle flow ~ 60%
Lithosphere topography and structure ~ 40%

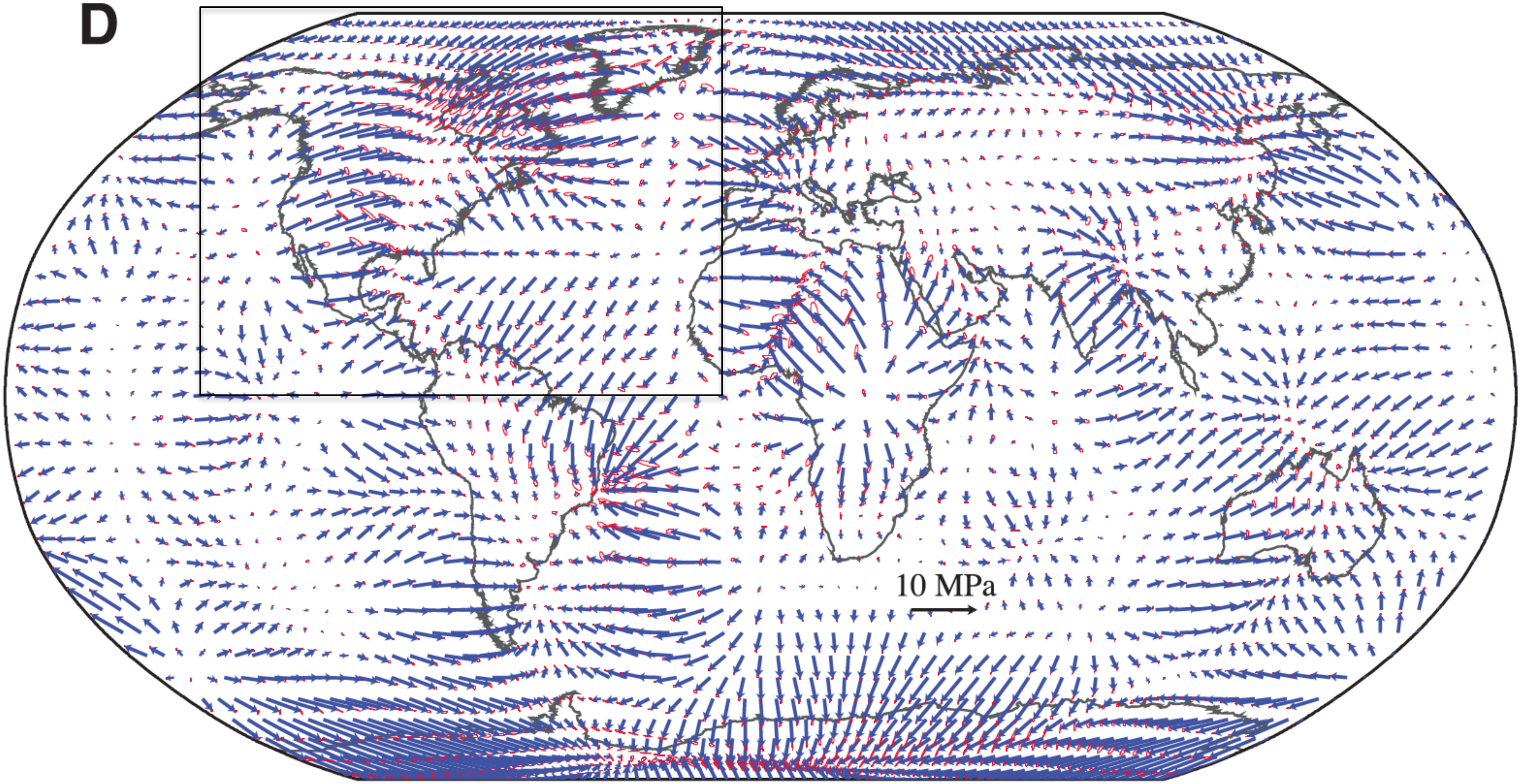

Tractions at base of lithosphere imposed by mantle flow
Ghosh and Holt [2012] *Science*

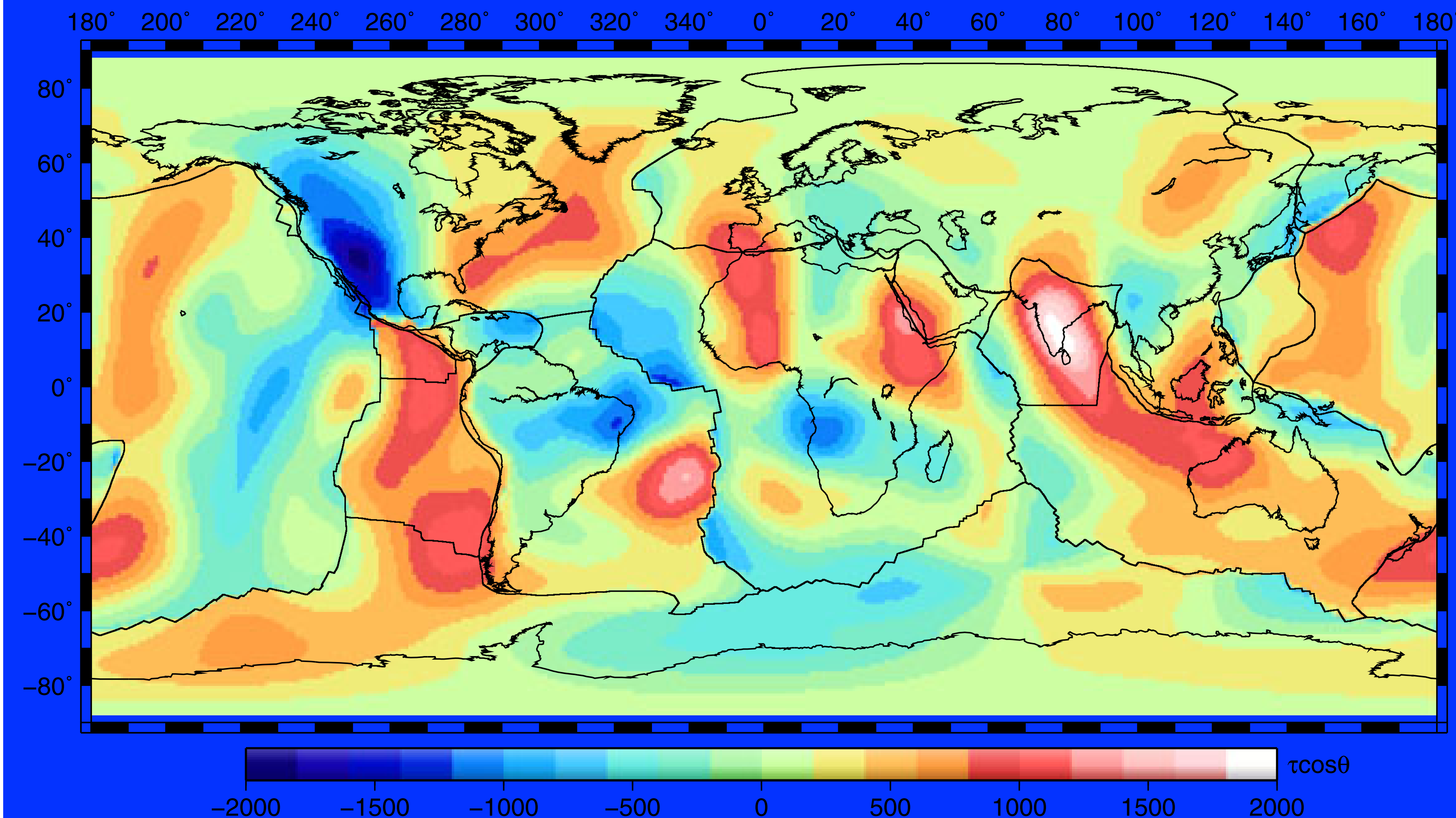

Tractions are both resistive and driving

Ghosh et al., JGR (2013)

Bottom Line

- Mantle leads the lithosphere (driving tractions) beneath major orogenic zones (Andes/Nazca, India, Eastern U.S.)
- Tractions integrate and provide important component to global force-balance of stress
- Observations require tractions 1-5 MPa, which provides traction-associated stresses that are of similar magnitude as GPE-associated stresses (1-4 TN/m).
- History of subduction is key in the mantle flow picture and therefore in global force balance
- Slabs, however, provide no stress guide effect that impact stresses within the plates

Bottom Line, Continued

- Depth integrated deviatoric stress magnitudes of 1-4 TN/m for plate boundary zones implies that weakening mechanisms (weak faults, presence of water in upper mantle, etc.) are required for strain accommodation within plate boundary zones.
- Rapidly deforming plate boundary zones are weaker than the more slowly deforming plate boundary zones